Journal of Hydrology 612 (2022) 128300

Contents lists available at ScienceDirect

Journal of Hydrology

journal homepage: www.elsevier.com/locate/jhydrol

Research papers

Climatic and hydrogeomorphic controls on sediment characteristics in the southern Sierra Nevada

Mohammad Safeeq [a,b,*], Aliva Nanda [c], Joseph W. Wagenbrenner [d], Jack Lewis [e], Carolyn T. Hunsaker [f]

[a] University of California, Division of Agriculture and Natural Resources, Davis, CA 95618, USA
[b] Civil and Environmental Engineering, University of California, Merced, CA 95343, USA
[c] Sierra Nevada Research Institute, University of California, Merced, CA 95343, USA
[d] USDA Forest Service, Pacific Southwest Research Station, Arcata, CA 95521, USA
[e] USDA Forest Service, Pacific Southwest Research Station (retired), Arcata, CA, USA
[f] USDA Forest Service, Pacific Southwest Research Station, Fresno, CA 93710, USA

ARTICLE INFO

This manuscript was handled by N. Basu, Editor-in-Chief, with the assistance of Genevieve Ali, Associate Editor

Keywords:
Sediment yield
Forest management
Paired catchment
Sierra Nevada
Snow transition

ABSTRACT

The magnitude of sediment yield from headwater catchments is controlled by the interactions among hydrology, geomorphology, and soil disturbance. In montane regions like the Sierra Nevada, snow is one of the main factors controlling the timing and magnitude of hydrological fluxes. However, the role of snow on modulating spatial and temporal variation of sediment yield remains unclear. Using 120-site years of sediment yield data from 10 headwater catchments (drainage area 50–475 ha), we examined the sediment yield characteristics across an elevational gradient (1,777–2,381 m elevation) in the southern Sierra Nevada. Across space and time, we calculated an average annual suspended sediment yield of 62 ± 147 Mg/km^2. In contrast, the measured mean annual bedload yield from the study catchments was small, 1.1 ± 2.4 Mg/km^2. A linear mixed-effects model showed that maximum annual discharge alone can only explain 24 % (marginal $R^2 = 0.24$) of the variance in sediment yield. Similarly, the hypsometric integral, which is often used as a metric for erosion susceptibility, showed no predictive power (marginal $R^2 = 0.005$). As much as 65 % of the variance in sediment yield can be explained by fixed effects when snow related drivers (i.e., center of flow timing and aspect) were included in the model along with maximum annual discharge, suggesting a strong influence of snowmelt. Moreover, the relationship between area normalized suspended sediment yield (Q_s) and unit discharge (Q) was significantly different between rain and snow events ($p = 0.001$). Both average slope (α) and exponent (β) terms of the $Q_s = \alpha Q^{\beta}$ relationship across the ten catchments were higher for rainfall ($\alpha = 5.8, \beta = 1.84$) than those for snowmelt ($\alpha = 3.1, \beta = 1.77$) events. As the erosion severity and power were higher during rainfall than the snowmelt events, a shift in the precipitation form from snow to rain under a warming climate will likely increase sediment yield. These results provide critical insights on background sediment yield in the southern Sierra Nevada and likely changes under future climate.

1. Introduction

Forested and snow laden mountains of the Sierra Nevada provide more than 60 % of California's developed water supply (Sierra Nevada Conservancy, 2014). Dams and reservoirs on the western slope of the Sierra Nevada play an integral role in bridging the timing mismatch between seasonal cycles of precipitation and water demand for California. Much of the mountain runoff, on average 29 km^3 (Dettinger and Anderson, 2015), is held behind dams during the rainy winter and early spring snowmelt before it is released to customers during the peak summer usage. However, these mountain streams across the United States are also major conduits for non-point source water pollutants such as sediment and nutrients that cause degradation of instream habitat quality and reservoir capacity (Kemp et al., 2011; Podolak and Doyle, 2015; Schleiss et al., 2016; United States Environmental Protection Agency, 2016a; United States Environmental Protection Agency,

* Corresponding author at: University of California, Division of Agriculture and Natural Resources, Davis, CA, 95618, and Civil and Environmental Engineering, University of California, Merced, CA 95343, USA.
E-mail address: msafeeq@ucmerced.edu (M. Safeeq).

https://doi.org/10.1016/j.jhydrol.2022.128300
Received 26 January 2022; Received in revised form 12 July 2022; Accepted 30 July 2022
Available online 6 August 2022

2016b). In the United States, half of the assessed (1,787,918 km or 31.4 % of the total waters) rivers and streams are classified as either threatened or impaired (United States Environmental Protection Agency, 2016a; United States Environmental Protection Agency, 2016b).

In California, nearly 90 % of assessed rivers and streams (340,397 km or 33 % of the total waters) are classified as water-quality impaired with temperature and sedimentation/siltation as the top two causes. Nearly 60 % of the assessed rivers and streams and 70 % of reservoirs, lakes, and ponds in California require determination of new Total Maximum Daily Loads (TMDL, United States Environmental Protection Agency, 2016a; United States Environmental Protection Agency, 2016b). Further, many California reservoirs are losing water storage capacity. Minear and Kondolf (2009) estimated as much as 2.1×10^9 m^3 of sediment deposited in California reservoirs between 1890 and 2008. This represents a loss of 4.5 % of the statewide total reservoir storage. The cumulative sedimentation is predicted to reach 7.1×10^9 m^3 by year 2200, which is 15 % of statewide reservoir storage capacity. This historic and future loss in reservoir storage alone is quite significant considering the removal cost and lack of flexibility for building additional storage (Lund, 2011, 2014). Increased water demand, curtailment of groundwater use, and decreased snow storage during winter months due to climate change will result in increased reliance on reservoir storage. These coarse scale estimates provide one view of sedimentation.

Evaluating background sediment yield, understanding site-scale variability in sediment transport, and identifying predictive variables for sediment yield such as geomorphology, land-use management, and climatic controls could improve management of reservoir sedimentation and achieve water quality standards (Borah et al., 2006; Costa et al., 2018). However, the past literature reported mixed observations on drivers of erosion and sediment yield. For example, catchment lithology and relief were found to be key drivers of sediment yield in basins with size less than 10^3 km^2 (Aalto et al., 2006; Andrews and Antweiler, 2012) but not in basins with size over 10^5 km^2 (Syvitski and Milliman, 2007). In the Rocky Mountains, Mueller and Pitlick (2013) found that the relative sediment supplies, in basins ranging between 1.4 and 35,000 km^2, were dominantly controlled by lithology and showed very little correlation to relief, mean basin slope, and drainage density. Stallman et al. (2005) reported a sharp contrast in sediment production between the geologic terrains of older Western Cascades and relatively young High Cascades where the former was represented by only 10 % catchment area but accounted for 62 % of the sediment yield. Similarly, Mueller et al., (2016) showed a strong relationship between sediment composition, i.e., suspended versus bedload, and lithology. The linkages between precipitation, temperature, and activation and cessation of runoff and sediment sources are also critical, especially in mountainous regions impacted by changing climate (Mano et al., 2009; Costa et al., 2018). The magnitude and intensity of sediment transfer associated with the snowmelt processes differ from rainfall-driven events. In the Mediterranean Region, where the snowmelt controls a major part of the discharge during spring and summer season, the transition in sediment regime from fine particle to coarser bedload was observed (Lana-Renault et al., 2011). Similarly, changes in land cover from forest management activities and/or wildfires can also alter the geomorphic regime (Safeeq et al., 2020).

Limited studies exist on long-term background sediment production rates in the Sierra Nevada. Riebe et al. (2000, 2001) investigated long-term erosion rates in the southern Sierra Nevada using cosmogenic nuclide data and found no correlation with climate and concluded that inferring patterns of sediment delivery using hillslope gradient alone can be misleading. At shorter time scales, sediment inputs to Lake Tahoe in the central Sierra Nevada have been studied extensively and show strong spatial and temporal variability due to differences in climate, geology, and land use (Coats et al., 2016; Carl, 1976; Langlois et al., 2005; Reuter and Miller, 2000; Simon et al., 2003). Studies in California's Coast Ranges go back to as early as the 1950s but focused mainly on documenting sediment yields associated with timber harvest and forest roads (Cafferata and Reid, 2013; Lewis et al., 2001; Richardson et al., 2020). Numerous field studies on post-disturbance, specifically post-fire, sediment delivery rates are also scattered spatially throughout the state (Cole et al., 2020; Olsen et al., 2021; Robichaud et al., 2013, 2008; Wohlgemuth et al., 2001). However, considering the range of variability in hydrology, climate, and geology in California, these studies provide limited specific applicability beyond their local landscapes. Looking at the 1,300 km^2 Lake Tahoe Basin alone, median suspended sediment yield varied by orders of magnitude between less than 0.5 Mg/km^2/year to as much as 14 Mg/km^2/year (Simon et al., 2003). This variability was largely controlled by the differences in precipitation and the amount of upstream disturbance.

The variations in sediment yield over space and time were even larger when looking across the Pacific Coast Region of the United States. At the smaller forested catchment scale with area between 0.02 and 16.2 km^2, reported sediment yields were found to vary by a factor of $\sim 10^4$ (0.05–550 Mg/km^2/year; Gomi et al., 2005). Across larger catchments and geomorphic regimes, O'Connor et al. (2014) analyzed data from a range of basins in northern California and Oregon, with size ranging from 0.6 to 6906 km^2, and reported bedload yields between 1.4 and 395 Mg/km^2/year. Similarly, Czuba et al. (2011) reported sediment yield variations between 1.3 and 584 Mg/km^2/year from the major rivers draining into Puget Sound and its adjacent waters (drainage area between 181 and 220,149 km^2). Looking at the sediment yield variations over time, Ambers (2001) reported sediment yield in the range of 38 and 244 Mg/km^2/year, with a long-term average yield of 98 Mg/km^2/year, from the 686 km^2 Dorena Lake watershed in the western Oregon. While the underlying hydrogeomorphic conditions in these studies are much different from those in the southern Sierra Nevada, these studies provide a basis for documenting and understanding locally relevant background sediment production.

Hydrologic landscapes of the Sierra Nevada are affected by climate, drought, and disease, resulting in tree mortality, wildfires, and other forms of disturbance that can alter the sediment regime. Wildfires are becoming more frequent, bigger, and more severe (Bedsworth et al., 2018). Warmer temperatures and loss of snowpack in the Sierra Nevada fuel the fires and alter the hydrology with higher rain-triggered winter peak flows (Safeeq et al., 2016; Westerling et al., 2006). The recent 2020 Creek fire, 2020 North complex fire, 2021 Caldor fire, and 2021 Dixie fire are examples of wildfire destruction in the source watersheds of California. This trend is projected to intensify in the future (Das et al., 2013; Huning and AghaKouchak, 2018), but its full range of geomorphic impacts is largely unclear with some indication that self-organization of channels may buffer the influence of climate signal evident in discharge (Goudie, 2006; Phillips and Jerolmack, 2016). The amount of active forest and fuel management, which is on the rise, is also modifying the landscape significantly (Gomi et al., 2005; North et al., 2015; Safeeq et al., 2020). Rachels et al. (2020) quantified the effect of forest harvesting on sediment sources in Oregon Coast Range headwater streams. They discovered that sediment loss from the harvested area was 10.6 times greater than streambank and 4.5 times greater than unharvested areas. Bywater-Reyes et al. (2017, 2018) showed catchment lithology and physiography as dominant controls on suspended sediment yield with catchments underlying friable lithologies and steeper slopes being more susceptible to erosion after contemporary forest management. Wise and O'Connor (2016) developed a spatially explicit suspended sediment yield model for western Oregon and found lithology and burned area, along with precipitation, explained 64 % of the variability in suspended sediment yield. Olsen et al. (2021) studied the effects of the 2013 Rim fire and post-fire salvage logging on rill connectivity and sediment yield in the Sierra Nevada. However, they did not find any significant change in mean rill density or log-transformed normalized sediment yield between logged and control catchments. Soil disturbance related to road construction or maintenance, timber harvest, and forest thinning or other management can also alter the erosion and sediment delivery dynamics of headwater streams (Rachels et al., 2020).

However, the impact of these anthropogenic and natural activities on landscape geomorphology varies with space and time.

The purpose of this research was to investigate long-term suspended and bedload sediment yields and assess underlying geomorphic and climatic controls. We analyzed suspended sediment concentration along with sediment load or yield due to their varying implications on aquatic and geomorphic processes. We utilized a unique dataset, with 120 site years (10 catchments * 12 years) of high-resolution sediment and discharge data, across an elevational gradient to answer the following research questions: 1) how does the sediment concentration and yield vary in space and time? 2) What are the key hydrogeomorphic and climatic controls on sediment yields in the Sierra Nevada? and 3) To what extent do forest management treatments (i.e., tree thinning and understory prescribed burns) affect sediment yields?

2. Materials and methods

2.1. Study area

The Kings River Experimental Watersheds (KREW), established in 2002, are active research sites located within the Kings River basin in the Southern Sierra Nevada of California (Fig. 1). KREW arecomprised of eight primary and two integrating catchments ranging in size from 0.5 to 4.7 km^2 (Table 1). Three primary catchments nest within each integrating catchment P300 and B200 (Fig. 1). The ten catchments are organized in two clusters across the rain-snow transition zone, consisting of the lower elevation Providence and higher elevation Bull sites (Fig. 2). Catchments at the Providence site drain to the Pine Flat Reservoir through Big Creek. Except for Teakettle (T003), catchments at

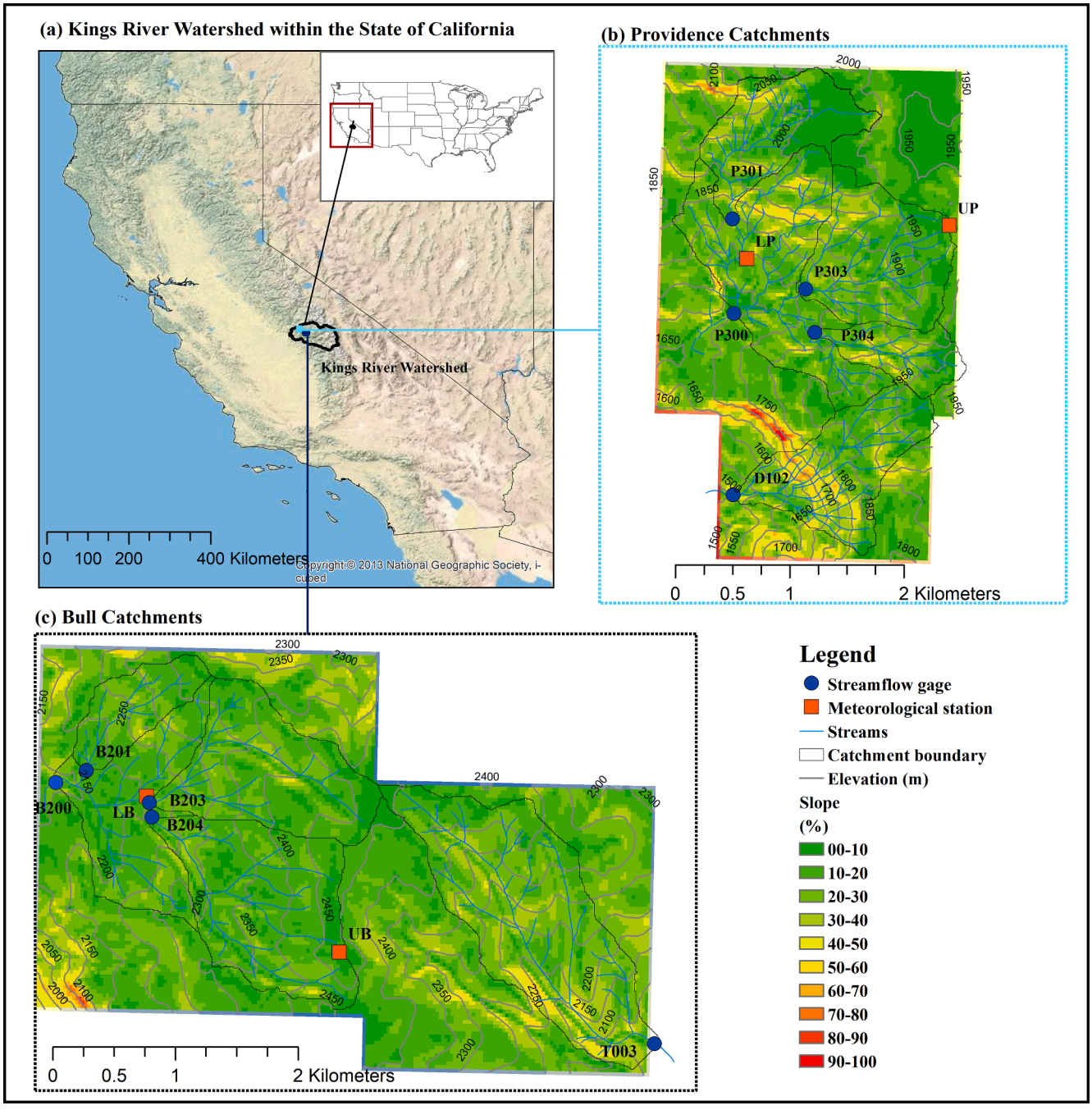

Fig. 1. Kings River Watershed within the state of California (a), lower elevation Providence (b) and higher elevation Bull (c) catchments in the Kings River Experimental Watersheds (KREW).

Table 1
Catchment characteristics for the Kings River Experimental Watersheds (KREW). Listed in order of increasing outlet-elevation.

Catchment	Forest Management Treatment	Area (km^2)	Elevation (m)	Relief (m)	Slope (%)	Aspect (deg.)	Hypsometric Integral (HI)	Drainage Density (DD) (km/km^2)	2011 Normalized Difference Vegetation Index (NDVI)*
Providence									
D102	Thinning (2012)	1.2	1777	482	37	241(SW)	0.581	10.1	0.69
P300	Integrating and Thinning	4.6	1872	372	26	190 (S)	0.538	7.4	0.68
P303	No-Treatment	1.3	1893	274	27	220 (SW)	0.567	7.4	0.69
P304	Control	0.5	1915	186	25	304 (NW)	0.649	6.9	0.69
P301	Thinning (2012)	1.0	1951	303	24	191 (S)	0.689	7.4	0.61
Bull									
B201	Thinning (2012)	0.5	2249	232	24	272 (W)	0.448	6.0	0.54
T003	Control	2.3	2260	412	31	122 (SE)	0.526	5.5	0.63
B200	Integrating, Thinning & Prescribed Fire	4.7	2327	358	23	201 (S)	0.544	5.2	0.51
B204	Thinning (2012) & Prescribed Fire (2013)	1.7	2373	249	21	224 (SW)	0.576	5.0	0.49
B203	Prescribed Fire (2013)	1.4	2381	288	23	227 (SW)	0.622	4.6	0.46

* Calculated using 30-m U.S. Geological Survey national land cover data. https://www.mrlc.gov/nlcd2011.php.

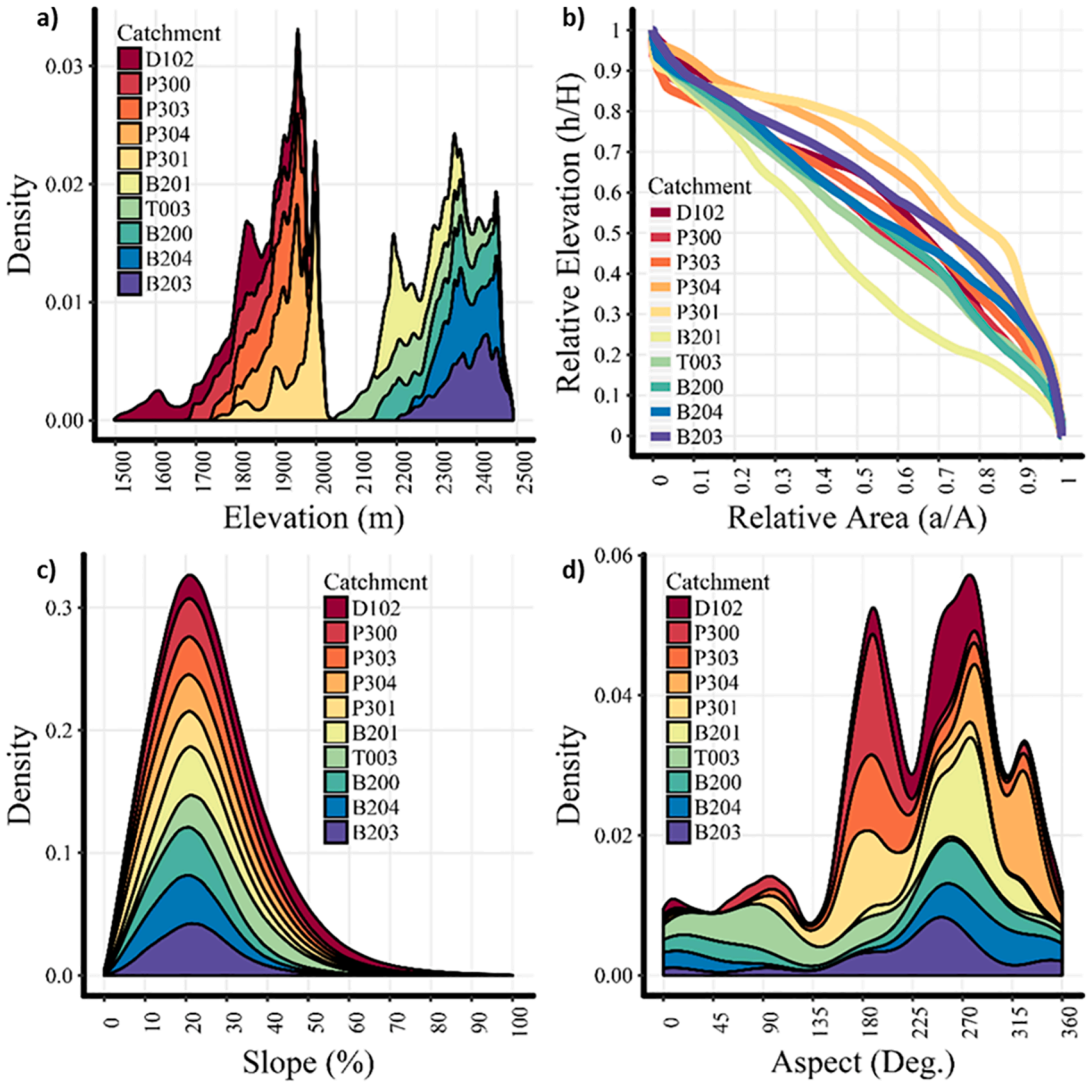

Fig. 2. Probability density functions of elevation (a), hypsometric curves (b), slope (c), and aspect (d) highlighting the differences in geomorphologically relevant topographic characteristics among the 10 study catchments. Variable a in the hypsometric plot represents the catchment area that lies at or above a given height h, A is the total catchment area and H is the total height estimated as the difference between maximum elevation and base elevation at outlet.

the Bull site drain to the North Fork of the Kings River through Dinkey Creek. T003 drains directly to the North Fork of the Kings River further upstream. The climate is described as Mediterranean with cold, wet winters and warm, dry summers. Long-term (1981–2010) average annual precipitation across the 10 catchments ranged from 1,026 mm in P300 to 1,234 mm in T003, and the mean daily air temperatures varied between 8 °C in B203 and 10 °C in D102 (Daly et al., 2008). The period of current research was 2004–2016 which includes the 2012–2015 drought (Supplementary Fig. S1). During the study period, mean annual precipitation of Bull and Providence was 1314 mm and 1208 mm whereas the mean annual air temperature was 10 °C and 7 °C, respectively. However, during drought years (2012–2015), the mean annual precipitation was 755 mm and 866 mm which is 46 % and 44 % less than the non-drought years (2004–2011 and 2016), for Providence and Bull, respectively.

The KREW catchments are underlain by Mesozoic granitic rocks in Providence and early Proterozoic to Cretaceous mixed rocks (mostly schist and gneiss) in Bull (Jennings et al., 2010). Regolith thickness is highest in Providence and constrained by temperature at higher elevations (O'Geen et al., 2018). Much of the Kings River Basin was glaciated during the Pliocene and early Pleistocene (Gillespie and Clark, 2011; Gillespie and Zehfuss, 2004; Kaufman et al., 2003). Well-drained Shaver and Gerle-Cagwin soils, hydrologic soil group B, dominate the lower elevation Providence and highly-drained Cagwin soils, hydrologic soil group A, dominate the higher-elevation Bull catchments (Hunsaker et al., 2012). The vegetation is characterized by mixed-conifer forest, primarily white fir (*Abies concolor*), ponderosa pine (*Pinus ponderosa*), Jeffrey pine (*Pinus jeffreyi*), sugar pine (*Pinus lambertiana*), and incense cedar (*Calocedrus decurrens*). Bull catchments contain a larger amount of red fir (*Abies magnifica*), in the range of 19–44 % (Hunsaker et al., 2012). Bare ground, which is mostly rock outcrop in the Bull catchments, accounts for 0–4 % of the land cover.

Hypsometric or area-altitude curves provide the relative area of a catchment to the relative elevation above the catchment mouth and can illustrate a range of conditions: inequilibrium (convex up) landform associated with diffusive dominated catchments, equilibrium (original), and monadnock (concave up) landform associated with fluvial dominated catchments (Strahler, 1952; Cohen et al., 2008; Vivoni et al., 2008). These curves can also be described as toeless to subdued concave up or type I, J-shaped or type II, and convex up or type III (Vachtman et al., 2013). Morphologically, all the catchments except B201 show convex up, mostly in the middle of the hypsometric curves indicating most erosion in the upper part of the catchment (Fig. 2). B201 shows a concave up hypsometry suggesting more erosion in the middle part of the catchment. The hypsometric integral (HI) is often used to quantitatively describe the geomorphic differences reflected in the hypsometric curve with higher HI values indicating more erosion susceptibility (Singh et al., 2008). The HI values across the ten catchments range between 0.448 for B201 to 0.689 for P301. Both Providence and Bull catchments can be classified as steep (Fig. 2) with an average slope ranging between 21 % in B204 to as much as 37 % in D102 (Table 1). Catchment aspect is dominated by south and west facing slopes. Estimated catchment drainage density varies between 4.6 km/km^2 in B203 to as high as 10.1 km/km^2 in D102, and generally increases with decreasing catchment elevation ($R^2 = 0.85$), increasing slope ($R^2 = 0.54$), and increasing vegetation cover ($R^2 = 0.64$) as inferred from the Normalized Difference Vegetation Index (NDVI) (Table 1).

2.2. Forest management treatments

The paired-watershed design of KREW was implemented to assess the impacts of two forest management treatments with a goal to better understand their impact on hydrology and geomorphology. The first phase of treatment was performed in the Providence and Bull catchments between July and November 2012. Timber harvest and mechanical thinning, using feller-bunchers and hand felling combined with ground-based skidding, were performed in P301, D102, B201, and B204 (Table 1) (Lydersen et al., 2019). In the second phase, prescribed fire was applied in Bull catchments B203 and B204 during fall 2013. The prescribed fire treatment was delayed in Providence catchments P301 and P303 because of unfavorable weather and ignition conditions. The subsequent prescribed burn in Providence occurred in late 2016 but falls outside of our analysis period. As a result, catchment P303 remained untreated during our analysis. Catchments P304 and T003 were the controls for Providence and Bull, respectively.

The forest management treatments at KREW were not very intensive, and had a negligible impact on basal area, canopy cover, and tree density (Lydersen et al., 2019). The thinning intensities of Providence and Bull were 23 trees/ha, and 33 trees/ha, respectively. Further, the thinning removed 4.5 m^2/ha and 4.6 m^2/ha basal areas from Providence and Bull catchments, respectively (Lydersen et al., 2019). However, the treatments were not applied uniformly throughout the catchments. In Providence, 71 % area was undisturbed after thinning, and 48 % area was found unburned after prescribed fire. Similarly, in Bull, 48 % and 61 % of the area were undisturbed and unburned after treatment, respectively. In terms of hydrologic response from these treatments, Bart et al. (2021) found a statistically significant increase in streamflow in Providence but not in Bull.

2.3. Data collection

2.3.1. Meteorology

Snow water equivalent (SWE) was measured at upper Providence (UP) and upper Bull (UB) at 15-minute intervals using rectangular snow pillows (Fig. 1). Each pillow consisted of four 1.2 × 1.5 m sections plumbed together and filled with non-toxic antifreeze and connected to a Sensotec® pressure transducer (Honeywell Inc., Columbus, Ohio). The pressure of the snow was converted to an equivalent water depth (SWE). Daily average SWE values were derived from 15-minute measurements (Safeeq and Hunsaker, 2016).

2.3.2. Streamflow

Streamflow was measured at 15-minute intervals using a combination of methods. Monitoring in the eight primary catchments began in fall 2003. The two integrating catchments, P300 and B200, were added in 2005 and 2006, respectively. All catchments except P300, B200, and T003 were equipped with dual Parshall Montana flumes constructed of structural fiberglass. An upstream small flume (8 or 15 cm throat width, 35.6 or 45.7 cm wall height) measured low flows and a downstream large flume (30, 61, 91, or 122 cm throat width, 91.5 cm wall height) measured high flows (Fig. 3). The distance between the two flumes varied from catchment to catchment and was less than 30 m. P300 was equipped with a 120-degree V-notch weir and T003 was gauged with a compound 90-degree V-notch and rectangular weir. The Teakettle Creek Experimental Forest was established in 1936 and the weir at T003 has been operational intermittently since 1938 (Kattelmann, 1989). For B200, discharge was estimated using a rating curve at a natural cross section. Submersible pressure transducers, manufactured by Telog® (Telog Instruments, Victor, New York), Solinst® (Solinst Canada ltd., Georgetown, ON) or Aquarod™ (Advanced Measurements and Controls, Inc., Camano Island, Washington), were installed inside a stilling well connected to the large flume where available, otherwise placed directly in the stream. Similarly, Teledyne Isco® air bubbler modules (Teledyne Isco, Lincoln, Nebraska) were connected to small flumes where available, otherwise placed directly in the stream. Manual discharge measurements were conducted using a Sontek® FlowTracker acoustic doppler velocimeter (FlowTracker, San Diego, California) across a range of flows (0.0023 m^3/s to 0.19 m^3/s) for developing the rating curve for B200.

2.3.3. Suspended sediment

Starting in fall 2006, stream water samples were collected at each

Fig. 3. Parshall Montana flumes, small flume in the foreground and large flume in the background, looking downstream, in B201 (top). An empty sediment pond with pond liner and log structure, looking upstream in B204 (bottom).

site using Teledyne Isco® model 6712 24-bottle sequential pump samplers (Teledyne Isco, Lincoln, Nebraska). Water samples were retrieved for laboratory analysis on a bi-weekly basis, or sooner when necessary and weather permitted. Grab samples were also collected when possible; however, most of the water samples for the analysis came from the automated samplers. Stream stage was used to initiate sampling. When the stage values rose to a pre-specified level, it triggered the pump sampler to begin sampling at a fixed time interval, typically one sample every 15–30 min. The trigger threshold values were manually adjusted frequently to account for seasonal changes in flow regime.

Across all sites and years (2006–2016), 1,267 water samples were collected and analyzed for suspended sediment concentration in the USDA Forestry Sciences Laboratory, Fresno CA. However, 41 samples were marked as erroneous due to negative suspended sediment concentration values and removed from the analysis. All the water samples were processed within seven days of collection to avoid biological growth. First, all water samples were filtered using glass fiber filters (1.0 μm pore size) and a vacuum pump (ASTM D 3977–97). Both filters and vacuum pump assemblies were rinsed using deionized water, then filters were placed in an aluminum pan and oven dried at 105 °C for 2 h. Oven-dried filters were placed in a desiccator for overnight cooling before taking the dry weight and subsequent vacuum filtering of water samples. Materials greater than 6 mm in any dimension (length or width) were removed from the filter. The filters with suspended sediment were oven heated to 105 °C for at least 2 h before placing them again in a desiccator for overnight cooling and recording the dry weight. The mass of suspended solids was calculated by subtracting the weight of the clean dry filter and aluminum pan from the total (dry filter, aluminum pan, and sediment) weight. Finally, we divided the mass of suspended solids by the volume of water sample to calculate the suspended sediment concentration (*SSC*, mg/L).

2.3.4. Bedload sediment

Sediment and organic matter deposits from the eight primary catchments were measured annually using lined settling ponds. These settling ponds were in natural deposition areas of the channel immediately below the large flume (Fig. 3), except at T003 where a permanent concrete-walled weir pond with a storage capacity of 200 m^3 was constructed in 1938. The settling ponds at the remaining sites were lined with 0.5 mm rubber pond liners and varied in storage capacity between 12 and 40 m^3. For the annual bedload sediment collection, streams were diverted, settling ponds were drained and emptied. The wet pond deposits were weighed in buckets to the nearest 0.5 kg. Volume-proportional sub-samples were collected for determining the dry mass, percent organic matter, and particle size distribution. Organic matter was separated into three different classes: (i) large organic matter such as sticks (>1 cm diameter and 10 cm length); (ii) coarse organic matter such as twigs, needles, sticks, bark, cones (size less than large organic matter but large enough to extract with tweezers); (iii) fine organic matter such as wood fragments (size equivalent to sediment). Large and coarse organic matter were separated from the pond material before the sediment was removed and the dry weight was determined in the laboratory. The fine organic matter fraction was determined by loss on ignition (24 h at 500 °C) of an oven-dried subsample of the sediment (Eagan et al., 2007; Hunsaker and Neary, 2012). Particle size distribution was determined for representative samples of the oven-dried mineral fraction following a standard sieve analysis using 2, 1, 0.5, 0.25, 0.125, and 0.065 mm sieve sizes (Eagan et al., 2007). Because of the difficulty in separating the deposited suspended sediment from the bedload sediment in the mineral fraction deposited in the ponds, we assumed that all the mineral fraction was bedload sediment. Trapping efficiencies of these settling ponds were not measured but, inferring from other studies, it may have been as low as 50 % during high discharge events (Richardson et al., 2020; Verstraeten and Poesen, 2001). Further information on meteorological, streamflow, and sediment measurements and quality control are available in earlier publications (Hunsaker and Safeeq, 2017; Safeeq and Hunsaker, 2016; Wagenbrenner et al., 2021a).

2.4. Sediment rating curves and yields

Suspended sediment rating curves were developed in the R environment (R Core Team, 2020) for each site by regressing the catchment area (*A*) normalized suspended sediment concentrations (*SSC/A*) (mg/L/km^2) from the samples against a range of flow metrics as explanatory variables (Table 2, Fig. 4). Ideally, these rating curves should be developed separately for pre- and post-treatment periods to account for any shift in the relationship between sediment and explanatory variables due to treatments. However, we felt that the highly unbalanced sample size for pre- and post- treatment observed suspended sediment data was problematic for developing separate rating curves at individual sites (Supplementary Fig. S5). The explanatory variables included in the rating curves were corresponding discharge, lagged discharge (by 2, 3, 4, 6, and 24 h) (L/s), day (time of water year as a decimal starting October 1, mid-night as zero), and Fourier sine and cosine series of sample date-time using 'smwrBase' package with $k.\max = 1$ (Lorenz, 2015). With the exceptions of day and Fourier sine and cosine series, all other explanatory variables were natural log-transformed and centered (Cohn et al., 1992) prior to building the model. Explanatory variable *day* was only centered, and Fourier sine and cosine series were used in the model without any data transformation. Also, since automated and grab samples were instantaneous while discharge was recorded at 15-min intervals, corresponding discharge values were extracted by linearly interpolating the two adjacent discharge values. An initial subset of 12 models were developed (nbest = 3, nvmax = 4) using the 'regsubsets' function (all possible subsets regression), from the 'leaps' package in R (Lumley and Miller, 2020). The *nbest* parameter identifies best performing, top 3 in this case, models and *nvmax* parameter sets the

Table 2
Summary of the least squared regression of log-transformed, area (A) normalized suspended sediment concentration (SSC/A) as a function of log-transformed corresponding (Q) and 2-hour (Q_2), 3-hour (Q_3),4-hour (Q_4), 6-hour (Q_6), and 24-hour (Q_{24}) lagged discharge, day-time of the water year (*day*), and Fourier transformed date-time describing one cycle of sine (*sinday*) and cosine (*cosday*) curves (Equation 1). With the exception of *sinday* and *cosday*, all explanatory variables were centered and all explanatory variables except day were log-transformed prior to building the model. *RSE* = residual standard error, R^2_{adj} = adjusted coefficient of regression, and n = number of samples. The values for the variables that were not significant are shown as blank in the table.

Catchment	*Intercept*	*Ln(Q)*	*Ln(Q_2)*	*Ln(Q_3)*	*Ln(Q_4)*	*Ln(Q_6)*	*Ln(Q_{24})*	*day*	*sinday*	*cosday*	RSE	R^2_{adj}	*n*
D102	3.66	1.50	−1.26		0.90	−0.57					0.81	0.53	122
P300	2.13	1.30		−0.37			−0.15			−0.51	0.87	0.61	167
P303	2.98	1.33	−0.33			−0.68				−0.856	0.81	0.58	91
P304	4.94	1.81	−0.41				−0.24		−0.43		0.85	0.60	229
P301	2.28	1.80	−3.14	2.73			−0.65				1.02	0.53	71
B201	3.40	1.31	−0.44				−0.33			0.58	1.03	0.57	94
T003	1.99	1.86	−1.11				−0.54		−0.18		0.52	0.75	86
B200	1.74	1.30	−0.30		−0.38		−0.26		0.26		0.77	0.54	126
B204	2.26	1.36				−0.43	−0.23	0.0035			0.92	0.68	125
B203	2.05	1.56	−0.26			−0.48		−0.0032			1.08	0.57	110

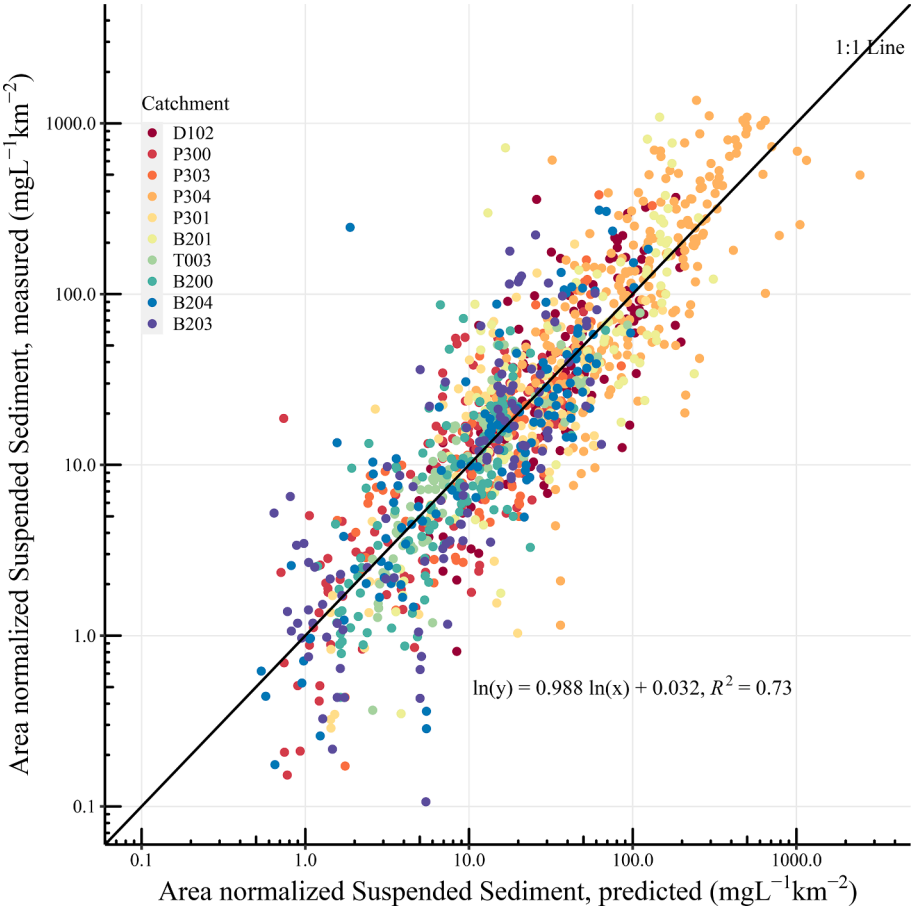

Fig. 4. Observed and predicted suspended sediment concentration using the rating curves described in equation [1] and Table 2.

maximum number of variables, in this case 4, that can be used in the model. The best regression model was selected based on ANOVA with statistical significance level $p < 0.05$, adjusted coefficient of regression, and Akaike information criterion (AIC). The relationship between *SSC* and Q for each catchment can be described, including all candidate variables, as:

$$\ln\left(\frac{SSC}{A}\right) = a + b.\ln(\boldsymbol{Q}) + c.\ln(\boldsymbol{Q}_2) + d.\ln(Q_3) + e.\ln(Q_4) + f.\ln(Q_6) + g.\ln(\boldsymbol{Q}_{24}) + h.(day) + i.(sinday) + j.(cosday) \quad (1)$$

where *SSC* = sediment concentration (mg/L), A = watershed area [km^2], Q = discharge [L/s], Q_n = discharge prior to n hours [L/s], *day* = day-time of water year [day], *sinday* and *cosday* = Fourier transformed date-time describing one cycle of sine and cosine curves for each water year, *a-j* = regression coefficients. The above-mentioned variables were used to take care of the annual seasonality (sinday and cosday), time trend (day), and flow dependence. The most frequently significant predictors are shown in bold. From this point onward, SSC_a is used as the acronym for area normalized suspended sediment concentration (mg/L/km^2).

Overall, predicted SSC_a using models developed from equation [1] explained 73 % of the variability in measured suspended sediment concentration (Table 2, Fig. 4). At the individual catchment level, adjusted coefficients of determination were between 0.53 for catchment D102 & P301 and 0.75 for catchment T003 (Table 2). SSC_a was

positively related to ln(Q), suggesting an increase in one will lead to an increase in another, and vice versa. With few exceptions, SSC_a was negatively related to the lagged discharge values that indicates a delayed response in which either SSC_a declined along the recession limb after a peak discharge or increased along the rising limb. Derived suspended sediment rating curves for each catchment were applied to 15-min discharge measurements and other related explanatory variables (Table 2) to create a continuous record of SSC_a. Area normalized suspended sediment yields (Mg/km^2) were calculated by first estimating the sediment flux Q_s (mg/s/km^2) by multiplying the SSC_a (mg/L/km^2) with the corresponding 15-min discharge Q (L/s). We then aggregated the 15-minute suspended sediment flux values by water year to derive annual suspended yields and added the corresponding annual bedload yields to derive annual total sediment yields for each catchment.

2.5. Climatic and hydrogeomorphic controls on sediment yields

Effects of climate and other hydrogeomorphic variables on suspended sediment and total sediment yields were analyzed using two approaches. First, we used the power law relationship between area normalized instantaneous suspended sediment flux Q_s and discharge Q to compare the differences in the relationships between rain and snowmelt driven runoff events. The Q_s was used as opposed to a more typical $SSC_a \sim Q$ relationship to account for differences in dilution from disproportional peak and baseflow behavior between rain and snowmelt events. Power law relationships took the form:

$$Q_s = \alpha(Q/A)^{\beta} \quad (2)$$

where Q_s [mg/s/km^2] is area normalized and flow weighted SSC_a, Q/A is discharge per unit area (L/s/km^2), and α and β describe the erosion severity and erosive power respectively (Asselman, 2000). The β parameter is usually greater than one, indicating an exponential effect of Q on sediment transport. A typical range of β parameter for suspended sediment transport range from 1.42 to 2.96 in different physiographic settings (Morehead et al., 2003).

Sediment samples were grouped between rain and snow using the snow water equivalent (SWE) information from the two meteorological stations (Fig. 1). Storms and corresponding SSC samples were identified as rain when there was no measured snow water equivalent. Based on this criterion, 502 out of 1,267 samples were identified as rain and 765 as snowmelt. SWE data from UB were used for Bull catchments and UP for classifying Providence catchments. We recognize that some of the SSC samples classified as snowmelt driven may also have included rainfall (e.g., rain-on-snow events) (Guan et al., 2016).

Second, we used a linear mixed-effects model to explore the hydrogeomorphic controls on the total (i.e., suspended and bedload) sediment yield from the KREW catchments. Prior to building the model, annual total sediment yield data were log-transformed to approximately normalize the error term. Fixed effects in the model were annual maximum discharge (Q_{max}), center of flow timing (*CT,* defined as the day of water year by which 50 % of the annual flow had passed the gauge) and catchment aspect (*Aspect*) to capture the precipitation regime and variability in snow among catchments. Hypsometric integral (*HI*) was included as a geomorphic control. Catchment elevation, relief, slope, drainage density, and NDVI were also explored but none of these variables were statistically significant predictors of annual total sediment yield. Similarly, annual minimum and average discharge were also explored but eventually left out in favor of Q_{max}. Catchment IDs were treated as a random effect in the model. We used the 'MuMin' package (Barton and Barton, 2015) in *R* for estimating coefficients of determination to describe marginal variation in sediment explained by the fixed effects and conditional variation in sediment explained by both fixed and random effects (Bywater-Reyes et al., 2018).

3. Results

3.1. Suspended sediment concentration

The area normalized suspended sediment concentration (SSC_a) between 2007 and 2016 varied by at least three orders of magnitude at each location (Fig. 5). The average SSC_a were lower in the high elevation Bull catchments (39 ± 92 mg/L/km^2) as compared to low elevation Providence catchments (98 ± 195 mg/L/km^2). Looking at individual catchment groups, the highest SSC_a in Providence was in P304 followed by D102, and both were significantly greater than the other three Providence catchments (Fig. 5c). At Bull, SSC_a was highest in B201 and significantly different from the rest of the catchments (Fig. 5d). The catchments at the Bull site were more similar than the catchments within the Providence site. The integrating catchments in Providence and Bull (P300 and B200, respectively) had the lowest SSC_a, and the SSC_a for P300 was significantly lower than all other Providence catchments (Fig. 5c).

Both catchments received fall rain along with several rain on snow events throughout the winter wet season (Neiman et al., 2008). Discharge in Bull mainly originated from snowmelt and peaked in mid-May (Supplementary Fig. S2). In contrast, the peak snowmelt discharge in Providence was usually-two weeks earlier. The SSC_a in Bull catchments were more variable from month to month than those in Providence with two distinct peaks in October and January (Supplementary Fig. S3). Both catchment groups showed relatively high SSC_a during early fall rain flush. There was also a noticeable lag between the timing of peak SSC_a and peak discharge in Bull but not in Providence. Highest SSC_a in Bull, after the fall flush, occurred in January as compared to peak discharge in mid-May. Peak timing of the sediment flux Q_s (SSC_a × instantaneous discharge Q) in Providence coincided with the average center of flow timing (i.e., around March) as opposed to coinciding with peak snowmelt discharge in Bull (Supplementary Fig. S4).

The sediment production characteristics in terms of erosion severity (α) and erosive power (β) were highly variable between and within the two catchment groups (Table 3). Overall, combining data from all catchments within each group, the α parameter was higher in Providence (5.92) as compared to Bull (2.39). In contrast, the β parameter in Providence (1.67) was very similar to that in Bull (1.68). However, this pattern was not consistent in individual catchments, suggesting a strong spatial variability within a catchment group. Looking at the α and β coefficients between rain and snowmelt flow types across all catchments, we found a statistically significant difference ($p = 0.001$, based on one-way ANOVA) in the intercept (i.e., α) of the sediment production-discharge relationships [2] between rain and snowmelt events. The difference in the slope of the linear regression (β) between rain and snowmelt events was not statistically significant ($p = 0.66$). At the individual catchment group level, both slope and intercept of the linear regression were statistically similar ($p > 0.22$) between rain and snowmelt events in Bull. However, the opposite was true for Providence. The α coefficients from the combined models in each catchment group ranged from 11.0 for rain to 2.8 for snowmelt in Providence and 1.94 for rain and 1.29 for snowmelt in Bull. In contrast, the β coefficient was 1.57 for rain and 1.85 for snowmelt in Providence and 1.90 for rain and 1.79 for snowmelt in Bull. In all Providence catchments, the α coefficients were higher for rainfall and the β coefficients were higher for snowmelt. This effect of storm type in Bull was highly variable between catchments but, in the regressions combining all Bull catchments, both α and β coefficients were greater for rainfall events (Table 3).

3.2. Total sediment yield

The average annual total sediment yield in Providence (85 Mg/km^2) was twice as much as in Bull (42 Mg/km^2). Annual total sediment yield was highly variable (standard deviation, 148 Mg/km^2) across all sites and years (Fig. 6). Additionally, as compared to Bull (standard

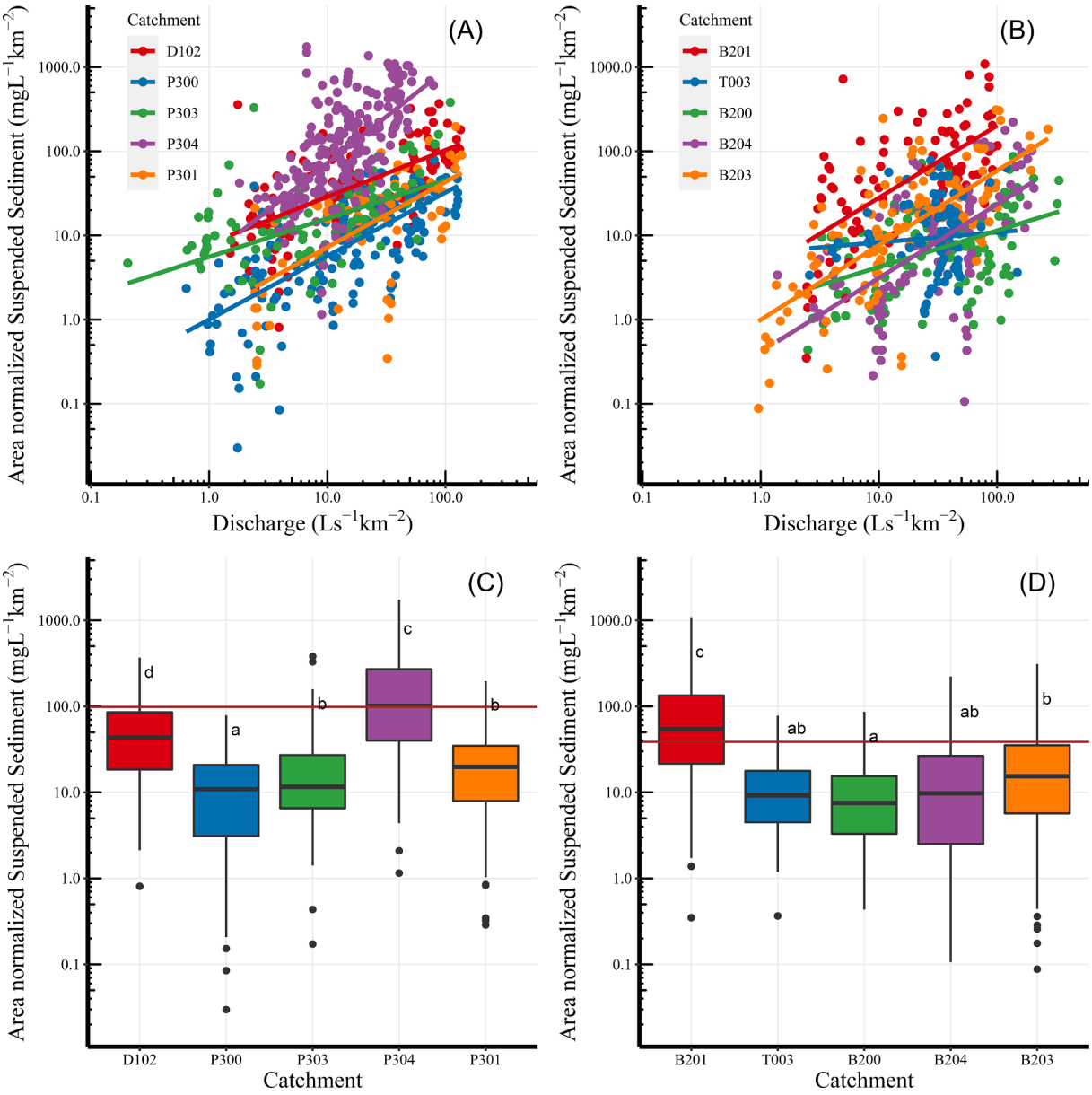

Fig. 5. (Top) Suspended sediment concentration and discharge relationships for the rain driven Providence (A) and snowmelt driven Bull (B) catchments for 2007–2016. (Bottom) Variability in the suspended sediment concentration among the different Providence (C) and Bull (D) catchments is shown as box plots. Each box plot shows distribution of data points representing outlier, minimum, 25 percentile, median, 75 percentile and maximum values. Horizontal orange lines show mean sediment concentration across the 5 catchments in each group and letters indicate Tukey's Multiple Comparison results. Catchments marked with same letters are not statistically different ($p > 0.05$). (For interpretation of the references to colour in this figure legend, the reader is referred to the web version of this article.)

deviation, 61 Mg/km^2), annual sediment yield in Providence (standard deviation, 200 Mg/km^2) was more variable from year to year. During 2004–2016, the highest sediment yield (1,074 Mg/km^2) was recorded in 2006, a relatively wet year (Supplementary Fig. S1), for P304, while the lowest sediment yield (0.1 Mg/km^2) was recorded in P301 in 2015 during a multi-year drought. Average annual total sediment yield ranged between a low of 11.7 (T003) and a high of 240.8 Mg/km^2 (P304) across the 10 catchments (Table 4). The contribution of bedload to the total sediment yield was fairly small: 0.4 (P303) to 3.8 (P304) Mg/km^2, or ~ 1 to 7 % of total yield (Table 4).

Total sediment yield showed no significant statistical correlation ($p > 0.05$) with the selected geomorphic descriptors. Among the selected geomorphic descriptors, catchment aspect and hypsometric integral (*HI*) showed the highest partial correlations with the total sediment yield, 0.62 and 0.64, respectively. Catchment drainage density was a distant third with a partial correlation of −0.41. In terms of hydroclimatic descriptors, total sediment yield was significantly correlated with annual maximum discharge (Q_{max}) and center of flow timing (*CT*) with partial correlations of 0.27 ($p = 0.003$) and 0.53 ($p < 0.001$), respectively (Table 5).

The best mixed-effects model based on AIC ($Q_{max} + CT + aspect$) was able to describe 77 % of the variation in the annual total sediment yield (model 8 in Table 6, Fig. 7). The marginal and conditional R^2 explains the variance of mixed-effects model by fixed effects and by both fixed and random effects, respectively. All three variables in the best model are associated with the sediment yield directly or indirectly. The catchment aspect influences the energy flux of the landscape along with the soil moisture, runoff, and vegetation dynamics; thus, it has a strong impact on sediment yield estimation. Similarly, *CT* was linked to the highest observed sediment flux in Providence and 2 months lag was observed between *CT* and the highest observed sediment flux in the Bull catchment (Supplementary Fig. S3). Moreover, as can be seen from the

Table 3
Erosion severity (α) and erosive power (β) parameters along with least squares regression statistics for equation 2. (dendf = denominator degrees of freedom).

Catchment	α	β	R^2	F-Statistic	Dendf	α	β	R^2	F-Statistic	Dendf	α	β	R^2	F-Statistic	Dendf
Providence	All (Rain + Snowmelt)					Rain					Snowmelt				
D102	9.68	1.56	0.82	565	120	15.4	1.59	0.85	210	36	4.91	1.69	0.85	476	82
P300	4.62	1.75	0.84	859	165	7.32	1.65	0.86	385	65	1.82	2.00	0.83	475	98
P303	7.34	1.46	0.79	330	89	16.6	1.18	0.76	94	30	3.59	1.68	0.84	306	57
P304	2.75	2.11	0.69	511	231	3.56	2.12	0.65	197	105	1.39	2.27	0.75	362	124
P301	1.20	1.78	0.76	219	69	2.52	1.69	0.71	34	14	1.34	1.70	0.73	140	53
Combined (D102, P300, P303, P304, P301)	5.92	1.67	0.75	1998	682	11.0	1.57	0.76	820	258	2.8	1.85	0.77	1418	422
Bull															
B201	2.06	1.86	0.78	336	92	1.95	1.94	0.74	119	42	1.41	1.93	0.73	132	48
T003	14.3	1.12	0.36	47	84	4.77	1.77	0.82	54	12	11.2	1.16	0.26	24	70
B200	7.37	1.43	0.73	334	124	4.0	1.76	0.8	228	57	4.08	1.52	0.52	70	65
B204	1.66	1.89	0.83	586	123	2.23	1.93	0.85	326	57	0.59	2.09	0.84	327	64
B203	0.57	1.88	0.71	264	109	0.06	2.77	0.74	115	41	0.87	1.73	0.7	157	66
Combined (B201, T003, B200, B204, B203)	2.39	1.68	0.71	1329	540	1.94	1.90	0.72	566	217	1.29	1.79	0.68	689	321

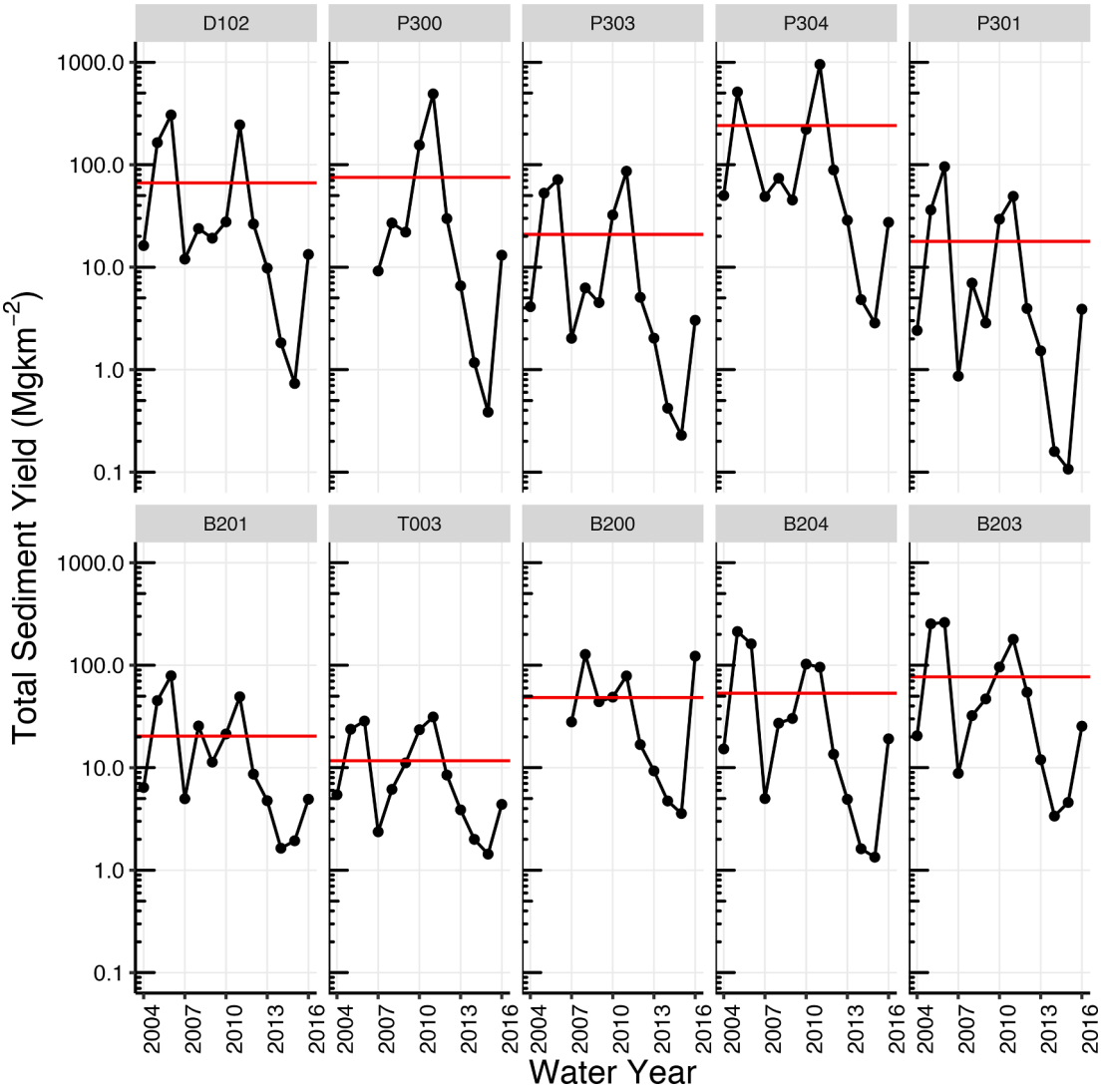

Fig. 6. Annual total (suspended and bedload) sediment yield by site, red lines show the mean value over the 2004–2016 water years. (For interpretation of the references to colour in this figure legend, the reader is referred to the web version of this article.)

Table 4
Means and standard deviations of annual estimated suspended, measured bedload, and total sediment yields from KREW catchments (2007–2016).

Catchment	Suspended (Mg/km^2)		Bedload (Mg/km^2)		Total (Mg/km^2)	
	Mean	Standard deviation	Mean	Standard deviation	Mean	Standard deviation
D102[a]	66	101	0.9	1.6	67	102
P300	76	153	na	na	na	na
P303	21	30	0.4	1.0	21	30
P304	237	364	3.8	5.4	241	370
P301	18	28	0.5	0.8	18	28
B201	20	23	0.8	1.0	20	24
T003[a]	11	10	0.8	1.2	12	11
B200	48	47	na	na	na	na
B204	53	68	0.5	0.8	53	69
B203	76	92	0.8	1.3	77	93

na Bedload sediment is not available for these sites.
[a] D102 does not flow into P300, and T003 does not flow into B200.

Table 5
Partial Pearson correlation coefficients between total sediment yield and hydroclimatic variables, Q_{min} = annual minimum discharge, Q_{mean} = annual mean discharge, Q_{max} = annual maximum discharge, and CT = center of flow timing. Statistically significant ($p < 0.05$) values are in bold.

	Log (*Total Sediment Yield*)	Q_{min}	Q_{mean}	Q_{max}	CT
Q_{min}	0.05	1			
Q_{mean}	0.00	0.70	1		
Q_{max}	0.27	−0.09	0.53	1	
CT	0.53	−0.22	0.46	−0.40	1

spread around 1:1 line (Fig. 7), the mean absolute error (40 Mg/km^2) was small with respect to the mean (60 Mg/km^2) and standard deviation (148 Mg/km^2). The model with Q_{max} (Model 1 in Table 6) as the only predictor was able to explain 44 % of the variation in the total sediment yield but only 24 % of the variation was explained by the fixed effect. The best single predictor model was for CT, a metric of snowmelt, which explained 68 % of the total variance (Model 2 in Table 6). Combining Q_{max} and CT (Model 5 in Table 6) resulted in the highest conditional R^2 with the two fixed effects explaining 55 % of the variance in the total sediment yield. Adding the aspect increased the variance explained by the fixed effects, from 55 % in model 5 to 65 % in this model (Model 8 in Table 6), but marginally lowered the conditional R^2. Surprisingly, adding the hypsometric integral (HI) did not improve the conditional R^2 of the Q_{max} and CT model (Model 5 in Table 6) or of the best model based on AIC (Model 8 in Table 6). Both HI and aspect are constant within a catchment. Thus, variation of sediment yields due to these variables was accounted for by the random effect (i.e., catchment). Specifying HI and aspect as fixed-effects shifts some of the random effects over to the fixed portion of the model, increasing the marginal but not the conditional R^2 (e.g., compare models 8 and 9 with model 5).

3.3. Effects of forest management on sediment

The association between forest management and area normalized suspended sediment concentrations (SSC_a) were analyzed by adding a dummy variable (pre-treatment = 0 and post-treatment = 1) and its interaction with discharge term, ln(Q), in equation [1]. Effects of forest management were evident in some catchments at both Providence and Bull sites (Supplementary Table S1). In Providence, both the treatment term and its interaction with discharge were statistically significant ($p < 0.05$) for D102 and P300. For P301, only the interaction term was statistically significant. In Bull, only the treatment term was statistically significant for B201 and B204 and just the interaction term was significant in B200. Neither the treatment nor the interaction term was statistically significant ($p > 0.05$) for B203 that received prescribed fire treatment only.

As mentioned previously, skewed sampling of SSC towards the post-treatment period (Supplementary Fig. S5) may influence the robustness of our catchment-level forest management impact analysis. To overcome this, we combined all the data by site, i.e., Providence and Bull, and performed linear mixed- effects modeling starting with the same variables as in Table 2 and adding a dummy treatment variable (pre-treatment = 0 and post-treatment = 1) and its interaction with discharge, ln (Q). This site-based analysis showed a statistically significant difference in SSC_a between pre- and post-treatment periods in Providence but not in Bull (Supplementary Table S2). For Providence, we found that both the treatment term and its interaction with discharge were statistically significant ($p < 0.05$). However, the negative coefficients suggest that the shift in the rating curve may have been driven by the drought rather than forest management. Under similar discharge conditions, forest management is expected to increase sediment production from increased supply while drought would likely reduce sediment production.

Effects of forest management on total annual sediment yield, suspended and bedload, were analyzed after adding the treatment impact as a dummy variable in the best mixed-effects model (model 8). Adding the treatment as an additional explanatory variable of total annual sediment yield significantly improved the model fit ($X^2 = 14.19$, $p < 0.001$), suggesting a significant shift in the total sediment yield during the post-treatment period. The AIC decreased by 12.2 with marginal and conditional R^2 values rising slightly to 0.68 and 0.78, respectively.

Another technique to evaluate the treatment effects on sediment is to compare the slope of observed sediment yields for treated and control catchments during pre- and post-treatment years (Fig. 8, Table 7). Regression slopes of treated versus control sediment yields increased after treatment, suggesting an increase in post-treatment sediment yield relative to control (except for P303 which received no treatment). Also, the shifts in slope for thinned catchments were small, suggesting a greater influence of prescribed fire on sediment yield than thinning. However, none of these shifts in regression slope were statistically significant ($p > 0.05$). Because of the drought in 2012–2015, post-treatment sediment yields in the controls (i.e., P304 and T003) were

Table 6
Explanatory power and significance of fixed and random effects in linear mixed models of total annual sediment yield using catchment variables, Q_{max} = annual maximum discharge (fixed), CT = center of flow timing (fixed), HI = hypsometric integral (fixed), *Aspect* = catchment aspect (fixed), d.f. = degree of freedom, and AIC = Akaike information criterion.

Model No.	Model predictors	d.f.	AIC	Log-likelihood	X^2 (Chi_{sq})	$P_r(>X^2)$	Marginal R^2	Conditional R^2
1	Q_{max}	120	467	−229			0.24	0.44
2	CT	120	404	−198	62.4	<0.001	0.45	0.68
3	HI	120	496	−244	0.00	1.000	0.00	0.15
4	*Aspect*	120	492	−242	3.87	<0.001	0.07	0.15
5	$Q_{max} + CT$	119	367	−178	128	<0.001	0.55	0.79
6	$Q_{max} + HI$	119	468	−229	0.00	1.000	0.25	0.44
7	Q_{max} + *Aspect*	119	462	−226	6.18	<0.001	0.31	0.40
8	$Q_{max} + CT$ + *Aspect*	118	361	−175	103	<0.001	0.65	0.77
9	$Q_{max} + CT$ + *Aspect* + HI	117	363	−174	0.33	0.56	0.66	0.77

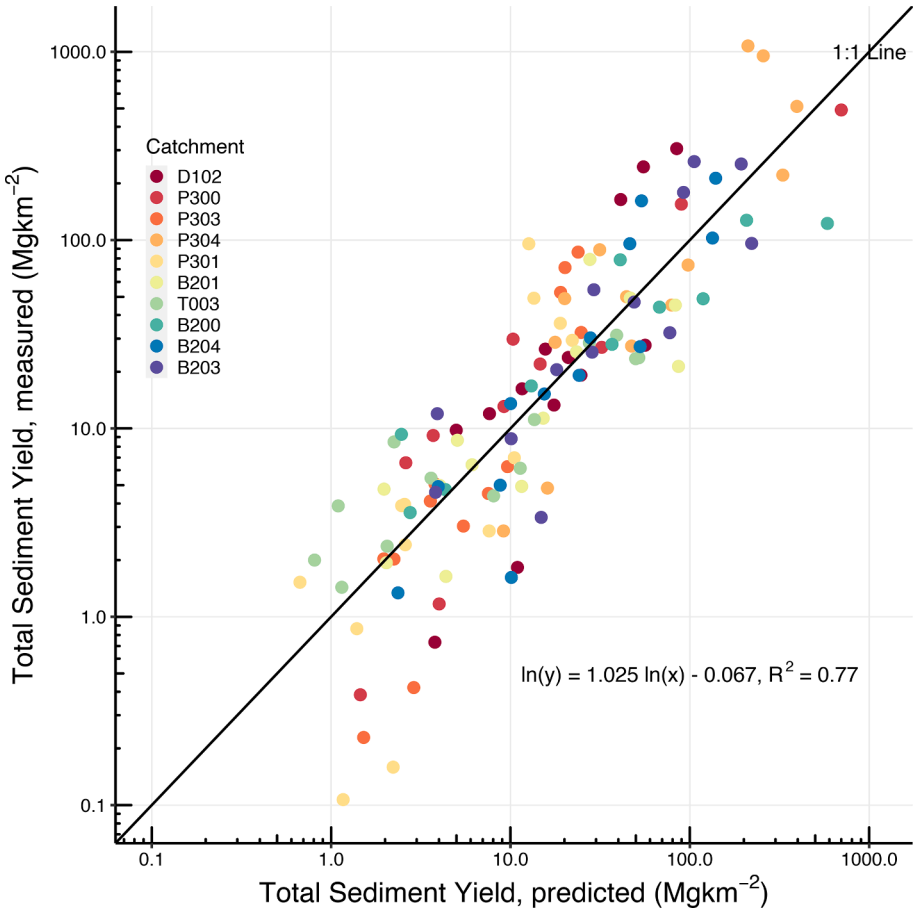

Fig. 7. Measured versus predicted annual total sediment yields. Predicted values were from the best linear mixed-effects model using Q_{max}, *CT*, and *Aspect* (model 8, Table 6) as the fixed effect predictors of sediment yield.

lower than their pre-treatment yields, with very little to no overlap in range (Fig. 8); therefore, it is possible that the slope shifts are merely indicative of non-linear relationships and drought rather than being treatment effects. In terms of changes, observed post-treatment sediment yields were higher by 27 % (D102) and 28 % (P300) (Table 7), relative to those estimated by the pre-treatment regressions (treated versus control). In P301, post-treatment observed sediment yield was 72 % lower than those estimated by the pre-treatment regression. In Bull catchments, observed post-treatment sediment yields were higher relative to those estimated by the pre-treatment regression, by 2 % in B204, 3 % in B200, and 19 % in B204. In B201, observed post-treatment sediment yield was 36 % lower than those estimated by the model. It was interesting to see a substantial increase in the total sediment yield in P303, a catchment with no-treatment. Also, all of this increased sediment in P303 was generated in 2016, the first normal precipitation year after the 2012–2015 drought (Bales et al., 2018; Safeeq and Hunsaker, 2016). This further suggests that these changes in sediment yield may have been an artifact of the drought rather than the forest management treatments.

4. Discussion

4.1. Total sediment yield

The average annual total sediment yield value of 63 Mg/km^2 from the KREW catchments is within the range of reported values for forested catchments in California and other parts of the western U.S. (Anderson, 1954; Gomi et al., 2005; Patric et al., 1984). In the Sierra Nevada, average annual sediment yield from the Lake Tahoe basin ranged from 0.7 to 67.9 Mg/km^2 (Nolan and Hill, 1991). Catchments in the Lake Tahoe study are comprised of a mixture of volcanic, metamorphic, and granitic rocks with scattered unconsolidated sediments that are more erodible than the soils at KREW. One of the Lake Tahoe catchments, General Creek (drainage area of 19.3 km^2), has comparable geology (granitic) and climate (average annual precipitation = 1,270 mm and temperature 5.8 °C) to KREW and generated 17.6 Mg/km^2 (1981–1987) and 10.4 Mg/km^2 (1984–1987) of annual suspended sediment yield (Nolan and Hill, 1991), approximately 28 % and 17 % of the mean value at KREW, respectively. Analyzing the datasets of Richardson and Wagenbrenner (2020), the average total sediment yield for the North Fork of Caspar Creek was found to be 43 Mg/km^2. However, Caspar Creek is rain dominated (mean annual precipitation ~ 1200 mm) and relatively warmer than KREW catchments with underlying marine sandstone and shale (Cafferata and Reid, 2013; Richardson et al., 2020). Snowmelt driven systems produce less hillslope erosion and, as a result, lower sediment overall. The only KREW catchment that substantially exceeded the range for the Sierra Nevada was P304, which is a baseflow dominated stream (Safeeq and Hunsaker, 2016; Eagan et al., 2007) and has a mining history. Also, the presence of channel bedrock is more dominant in the other KREW catchments (Safeeq and Hunsaker, 2016). Turowski et al. (2011) suggest that even a small amount of bedrock exposure can make a stream act like a bedrock channel. Other factors such as low rock fraction in topsoil, low proportion of exposed granite, and ongoing down-cutting of channels have been reported as possible mechanisms for higher sediment yields in P304 (Stacy et al., 2015; Hunsaker and Neary, 2012; Eagan et al., 2007; Martin et al., 2009). P304 had the highest, by a factor of 4, coarse sediment or bedload yield among the studied catchments, providing the necessary tool for channel

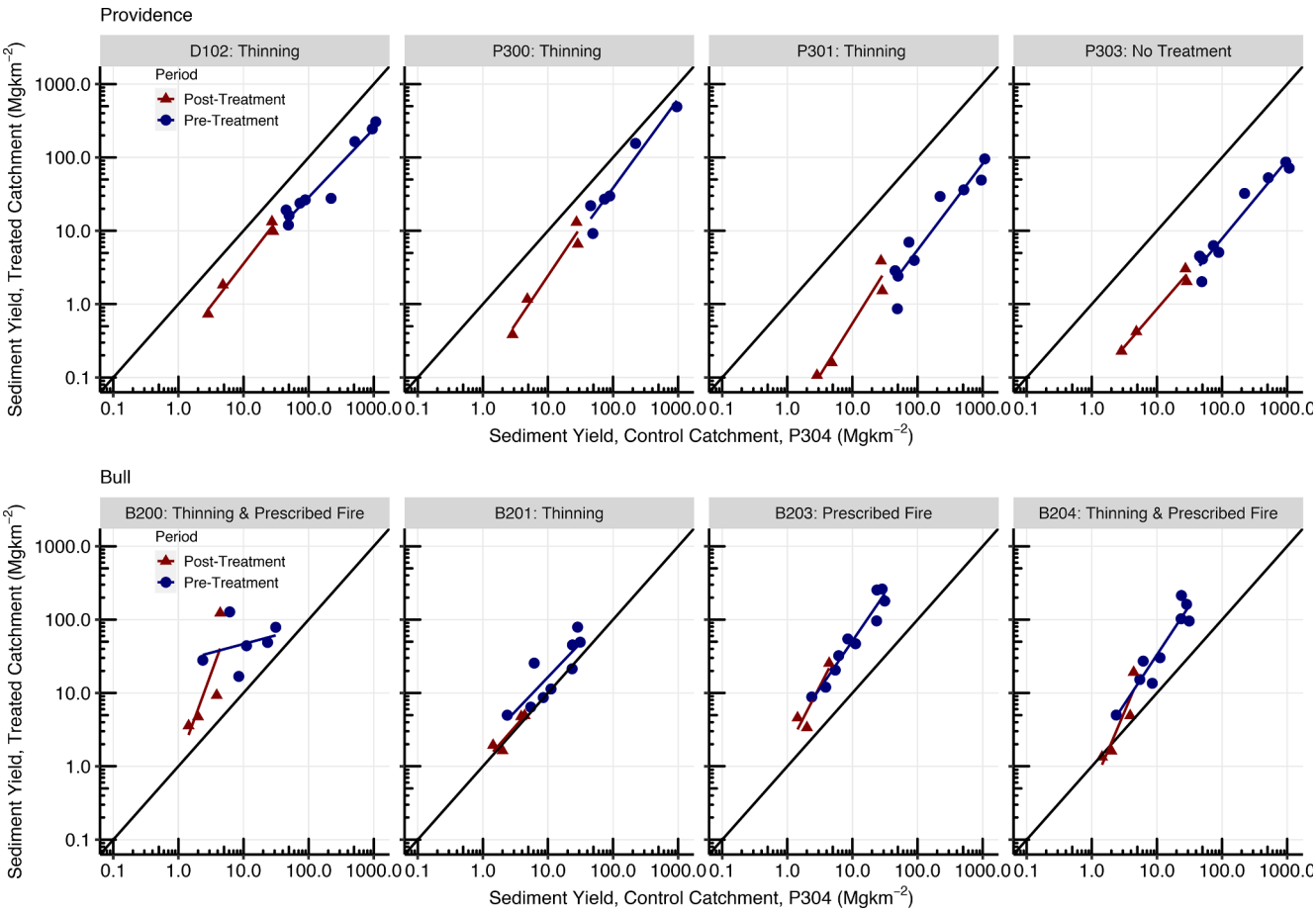

Fig. 8. Comparisons of pre- and post-treatment sediment yields between the treated (y-axis) and control (x-axis) catchments in Providence (top row) and Bull (bottom row). Circles and triangles are the observed data and solid lines represent best linear fits.

Table 7
Effect of forest management treatments on annual total (suspended and bedload)) sediment yield.

Catchment	Slope (Treated ~ Control)		Sediment Yield (Mg/km^2)			% Change[#]
	Pre-Treatment	Post-Treatment	Pre-Treatment (observed)	Post-Treatment (observed)	Post-Treatment (estimated)*	
Providence						
D102 (thinning)	0.93	1.15	93.4	6.4	5.0	27[b]
P300 (thinning)	1.22	1.32	122	5.3	4.5	19[b]
P303 (no-treatment)	1.07	1.03	29.4	1.4	1.1	28[b]
P301 (thinning)	1.18	1.42	25.3	1.4	5.0	−72[b]
Bull						
B201 (thinning)	0.93	1.01	28.0	3.3	5.2	−36[a]
B200 (thinning & prescribed fire)	0.24	2.43	57.3	35.1	34.1	3[b]
B204 (thinning & prescribed fire)	1.35	2.10	73.8	6.8	6.6	2[b]
B203 (prescribed fire)	1.30	1.72	96.5	11.1	9.4	19[b]

*Estimated using the pre-treatment regression between treated and control.
[#] Using post-treatment sediment as (observed-estimated) x100/estimated, a = statistically significant ($p = 0.10$), b = not statistically significant ($p > 0.10$).

incision in granitic catchments of the Sierra Nevada (Callahan et al., 2019).

Despite the high sediment yield in P304, which is one of the two smallest catchments, we found no relationship between suspended or total sediment yield and catchment area ($R^2 = 0.03, p = 0.6$). Catchment area and sediment yield are generally known to have a negative correlation (Griffiths et al., 2006). However, a positive correlation was also observed between turbidity and drainage area for 28 streams of the Coast Range of Northern California (Klein et al., 2012). A similar finding between sediment yield and area was observed in the North Fork of Caspar Creek before the disturbance in the experimental catchments (Lewis et al., 2001). The varying nature of this correlation is due to its dependency on multiple catchment variables, i.e., slope, vegetation cover, and soil type. Bedload yield at KREW was marginally correlated with the catchment area but statistically not significant ($R^2 = 0.24, p = 0.21$). Lack of correlation between sediment yield and drainage area at KREW suggests that erosion processes at this scale are highly complex. The transport limitation seems apparent when looking at the two integrating catchments, B200 and P300. Average annual total sediment yields from these two integrating catchments were only one-third of the total sediment yield generated by the upstream catchments. This shows a significant loss in sediment transport capacity as one moves

downstream to lower elevation with less steep slopes. While looking into individual catchments, the total sediment yields of P301 and P303 are lesser than the P300 due to their lean flow conditions. The ratio of steeper slopes to flat areas generally decreases with increasing catchment area as indicated by lower HI values for P300 and B200 (Table 1, Fig. 2).

4.2. Sediment yield and snow

Our results indicate a strong control of precipitation phase, i.e., rain vs snow, on measured SSC_a, suspended sediment flux Q_s (SSC_a × instantaneous discharge Q), and total (suspended and bedload) sediment yield. Effects of the precipitation phase on SSC_a, analyzed using a linear mixed-effects model after adding a dummy variable (snow = 0 and rain = 1) and its interaction with discharge, ln(Q), to the list of variables included in the sediment rating curve [1], showed a statistically significant ($p < 0.05$) positive association with the precipitation phase (Supplementary Table S2). In terms of sediment fluxes, measured Q_s for rainfall events were significantly ($p < 0.001$) higher than those for snow events under similar discharge. This was also evident in the values of α and β [2] between rainfall and snowmelt events. Higher values of α for rainfall events in Providence suggest higher erosion severity when compared with snowmelt driven events. However, snowmelt driven events have higher erosive power, indicated by higher values of β, when compared with rainfall events. In contrast, snow-dominated Bull catchments showed both higher erosion severity and erosive power during rainfall events (except for β in B204), indicated by higher α and β values for rainfall driven events than those under snowmelt. Further, it was observed that the measured suspended sediment fluxes were lower during April-June, the peak snowmelt season in Bull site particularly (Supplementary Fig. S4). These findings suggest a likely increase in SSC_a and Q_s as the catchments transition from more snow to rain. However, the overall impact on the total annual sediment yield will depend on the future runoff regime, both the magnitude and intermittency of runoff along with the availability of sediment. Currently, persistent higher discharge during the snowmelt season contributed on average 51 % (range: 43 % in P301 and 60 % in P301) and 63 % (range: 56 % in B200 and 72 % in B204) of the total suspended sediment yield in Providence and Bull sites, respectively. In the future, the extent of shifts in both runoff regime and sediment sources/availability remains highly uncertain. As discussed earlier, annual total sediment yield was positively correlated with Q_{max} and CT. Based on the historical observation, an earlier shift in CT would imply a reduction in annual total sediment yield. However, an increase in Q_{max} through more extreme precipitation or increased rain-on-snow events along with enhanced sediment supply between rainfall events as the catchments go through wetting and dry cycles can lead to an overall increase in total sediment yield.

Similar findings have been reported in other Mediterranean high mountain catchments of Spain (Lana-Renault et al., 2011). Mano et al. (2009) also stated the important role of snowmelt in transporting most of the suspended sediment (i.e., 50 %) in Mediterranean watersheds. Lana-Renault et al. (2011) also found the absence of bedload during snowmelt events due to insufficient energy of snowmelt runoff to move particle sizes greater than 2 mm. Hunsaker and Neary (2012), compared the bedload rates and changes in channel morphology and found as much as twenty times more sediment originating from streambanks than those from headcuts. Prolonged and consistent high flows, diurnal fluctuations, and increased turbulence during the snowmelt season are more likely to destabilize streambanks, scour the channel, and transport the solids in the water column or along the bed (Anderson et al., 2000) than short-lived rain-driven discharge events of similar magnitude.

As mentioned previously, the Providence catchments are in the rain-snow transition zone and precipitation phase at this location is highly sensitive to temperature (Klos et al., 2014; Safeeq et al., 2016). Soils in these catchments contain a significant portion of gravel (Johnson et al., 2011) which along with sand currently dominate the composition of the bedload (Hunsaker and Neary, 2012). In Bull catchments, the average gravel and sand content was 6–31 % and 67–88 %, whereas, for providence catchments, they varied in the range of 3–16 % and 76–81 %, respectively (Hunsaker and Neary, 2012). However, the average silt content of most of these catchments was less than 10 %, except for B201 (12 %), P303 (12 %), and P304 (16 %). An increase in temperature will lead to more prevalent rain-initiated runoff events, which in turn will likely mobilize more coarse sediment. This will also shift the timing of the sediment transport as the runoff timing shifts earlier in the season. Similar results also have been reported in an Alpine catchment (Costa et al., 2018) that the temporal shift in temperature changes the driving force of suspended sediment from ice melt and snowmelt to rainfall. The lack of snow on the ground surface increases the chance of erosion during heavy rainfall events. Annual bedload of Providence is better correlated with flood flows (Q_{max}, R^2 between 0.88 and 0.94) than average annual flows (Q_{mean}, R^2 between 0.75 and 0.91) or flow timing (CT, R^2 between 0.13 and 0.45), suggesting discharge pulses from snowmelt were incapable of moving coarse sediment downstream. This may be driven by a lack of supply as the bankfull discharge, common during the snowmelt season, generally exceeded the effective discharge (Nolan et al., 1987). As the snowmelt contribution to runoff diminishes, sediment production will be concentrated within the rainy season, typically between October-April (Safeeq and Hunsaker, 2016).

4.3. Effect of forest management

Our study found that the impacts of forest management on total sediment yield were confounded by the drought. Despite the observed changes in post-treatment runoff in Providence (Bart et al., 2021), changes in sediment yield with respect to control were within the same range as those observed in untreated catchment P303. The intensity of the treatments at KREW was relatively low and the impacts were distant from streams (Lydersen et al., 2019). Several catchments showed up to a 28 % increase in estimated sediment yield with respect to their control catchments. But these changes may have been an artifact of the 2012–2015 drought that coincided with the post-treatment period. In years soon after treatment, when treatment impacts are generally highest, many streams had low streamflow (Safeeq and Hunsaker, 2016), and had very little capacity to mobilize sediment.

Forest management activities with ground disturbance, such as the mechanical thinning and prescribed burning at KREW, were expected to increase sediment production (Gomi et al., 2005). Higher post-management sediment yields are often associated with an increase in sediment supply from excessive ground disturbance (Safeeq et al., 2020) and extreme rainfall events (Bathurst and Iroumé, 2014; Grant and Wolff, 1991; Rainato et al., 2017; Robichaud et al., 2016; Swank et al., 2001). Mechanical thinning in KREW was performed using a combination of feller-bunchers, hand felling, and ground-based skidding that was likely to disturb the soil and change soil physical properties (Solgi et al., 2016). Mechanical equipment was not allowed within 30 m of the stream bank; trees could be felled within 15 m of the stream and dragged out. Prescribed fire can also remove ground cover and alter soil properties like infiltration, leading to increased erosion (Certini, 2005; DeBano, 1991). It is likely that the lack of hydrologic drivers during prolonged drought allowed our catchments to recover from management related physical changes in the landscape. Similar results have been shown in post-wildfire conditions where drought after fires resulted in minimal response (Florsheim et al., 2017; Mayor et al., 2007; Wagenbrenner et al., 2021b).

4.4. Uncertainty

Implementation constraints associated with field experiments and monitoring can introduce uncertainty and are worth highlighting. Among these, the one with the largest impact on the results of this study involved sampling of suspended sediment. First, although stream

discharge measurements in primary catchments started in 2003, suspended sediment sampling did not begin until late 2006. Additionally, due to logistical and staffing constraints twice as many samples were collected between 2013 and 2016 than in the preceding six years with no sampling in water years 2011 and 2012 (Supplementary Fig. S5). This unbalanced sampling may have influenced our rating curves towards drought years. Having fewer samples during the pre-treatment period also limited our ability to develop separate pre- and post-treatment rating curves at the individual catchment level.

Second, the discharge range for suspended sediment samples across all catchments (0.00027–1.6 m^3/s) was well below the maximum observed discharge from KREW catchments (Supplementary Fig. S5). Except at B204, the highest sampled discharge values had recurrence intervals of less than 2.5 years. Although measured discharges above the upper limit of suspended sediment sampling were less than 1.5 % of all the 15-minute discharge records, their contributions to total suspended sediment yields were in some cases substantial. The percentage of suspended sediment yield generated from discharge above the upper limit of sampled discharge for suspended sediment ranged from 15 % in D102 to 58 % in P300 and 18 % in T003 to 43 % in B201. These high discharge events are often short-lived, hence challenging to sample. Although the automated ISCO samplers were set to trigger during high streamflow, a maximum of 12 samples could be taken during a high flow event. Nonetheless, considering the non-linear relationship between sediment flux and discharge [2], a paucity of sediment samples during these high discharge events may have caused underestimation of suspended sediment yields. Additionally, as mentioned earlier, the lower trapping efficiency of sediment ponds during high flows may have caused underestimation of bedload yield (Verstraeten and Poesen, 2001).

Third, suspended sediment for integrating catchments B200 and P300 may have been under-reported from the flow disruption by the instream flumes and settling of fine sediments in the upstream sediment ponds. Pond-deposited sediment, which includes some fraction of the suspended sediment (Richardson et al., 2020; Stacy et al., 2015) from the stream network above P300 and B200 were removed each year. The fraction of clay and silt in the bedload sediment upstream from P300 ranged between 56 % in P303 and 71 % in P304. Similarly, 39 % (B203), 44 % (B204), and 74 % (B201) of the sediment materials upstream from B200 were clay and silt (Stacy et al., 2015). However, considering the other sources of uncertainty (e.g., laboratory analysis, rating curves, sampling as discussed earlier) and the overall small contribution of bedload sediment to the total sediment yield, the influence of upstream sediment ponds probably was minimal.

5. Conclusions

Continuous discharge and sediment data from 10 headwater catchments in the southern Sierra Nevada allowed us to quantify the magnitude and spatio-temporal variability in background sediment yield and assess potential changes under future climate and forest management conditions. We showed that the background sediment yields in these catchments are comparable to reported values for forested catchments in California and other parts of the western United States. Although the headwater catchments were selected to have similar landscape characteristics and are adjacent to each other within the two sites, we found their average annual total sediment yields to be highly variable (ranging between 12 Mg/km^2 and 241 Mg/km^2). We also found the contribution of bedload sediment to the total sediment yield to be negligible. An undisturbed catchment in the Teakettle Experimental Forest (T003, part of the Bull site) had an estimated mean annual sediment yield of 12 Mg/km^2 (range 1.5–30 Mg/km^2) and can serve as a reference for background sediment yields in the southern Sierra Nevada. The area normalized measured suspended sediment concentrations of Bull and Providence were in the range of 39 $\pm$ 92 $mg/L/km^2$ and 98 $\pm$ 195 $mg/L/km^2$, respectively.

Catchment aspect, annual maximum discharge, and center of flow timing together were able to explain 77 % variance of the total (suspended and bedload) annual sediment yield. A statistically significant effect of precipitation phase (rain vs. snow) on the sediment-discharge relationship was also found. Loss of snowpack under a warming climate may increase the contribution of bedload sediment as the streams become flashier. Effects of forest management treatments were not significant and were confounded within the drought signal. Our study illustrated the challenges in paired-catchment based attribution analysis under varying climate conditions such as extreme droughts. This study provides the first long-term (10 years) suspended and bedload sediment results for multiple catchments with varying land use and management conditions in the southern Sierra Nevada. Additional research is needed to further improve our understanding of forest management impacts on erosion and sediment delivery at varying spatial and temporal scales and under different weather (climate) patterns.

CRediT authorship contribution statement

Mohammad Safeeq: Conceptualization, Methodology, Data curation, Writing – original draft, Visualization, Writing – review & editing. **Aliva Nanda:** Methodology, Visualization, Writing – review & editing. **Joseph W. Wagenbrenner:** Conceptualization, Supervision, Writing – review & editing. **Jack Lewis:** Methodology, Writing – review & editing. **Carolyn T. Hunsaker:** Conceptualization, Supervision, Writing – review & editing.

Declaration of Competing Interest

The authors declare that they have no known competing financial interests or personal relationships that could have appeared to influence the work reported in this paper.

Data availability

Data will be made available on request.

Acknowledgements

Funding for the Kings River Experimental Watersheds (KREW) project was provided by the USDA Forest Service, the USDI and USDA Forest Service Joint Fire Science Program, from California's State Water Resources Control Board, through Proposition 50 (Water Security Clean Drinking Water, Coastal, and Beach Protection Act of 2002), the California Department of Forestry and Fire Protection, and the Sierra Resource Conservation District. We thank the Sierra National Forest for their partnership and cooperation.

Appendix A. Supplementary data

Supplementary data to this article can be found online at https://doi.org/10.1016/j.jhydrol.2022.128300.

References

Aalto, R., Dunne, T., Guyot, J.L., 2006. Geomorphic controls on Andean denudation rates. J. Geol. 114, 85–99.

Ambers, R.K., 2001. Using the sediment record in a western Oregon flood-control reservoir to assess the influence of storm history and logging on sediment yield. J. Hydrol. 244 (3–4), 181–200.

Anderson, H.W., 1954. Suspended sediment discharge as related to streamflow, topography, soil, and land use. Eos, Trans. Am. Geophys. Union 35, 268–281. https://doi.org/10.1029/TR035I002P00268.

Anderson, J., Estabrooks, T., Mcdonnell, J., 2000. Duluth Metropolitan Area Streams Snowmelt Runoff Study. Minnesota Pollution Control Agency. https://www.pca.state.mn.us/sites/default/files/duluth-snowmeltstudy.pdf [last accessed 5/7/2022].

Andrews, E.D., Antweiler, R.C., 2012. Sediment fluxes from California coastal rivers: the influences of climate, Geology, and topography. J. Geol. 120, 349–366.

Asselman, N.E.M., 2000. Fitting and interpretation of sediment rating curves. J. Hydrol. (Amst) 234, 228–248.
Bales, R.C., Goulden, M.L., Hunsaker, C.T., Conklin, M.H., Hartsough, P.C., O'Geen, A.T., Hopmans, J.W., Safeeq, M., 2018. Mechanisms controlling the impact of multi-year drought on mountain hydrology. Scientific Reports 2018 8:1 8, 1–8. 10.1038/s41598-017-19007-0.
Bart, R.R., Safeeq, M., Wagenbrenner, J.W., Hunsaker, C.T., 2021. Do fuel treatments decrease forest mortality or increase streamflow? A case study from the Sierra Nevada (USA). Ecohydrology 14, e2254.
Barton, K., Barton, M.K., 2015. Package 'mumin.' Version 1, 439.
Bathurst, J.C., Iroumé, A., 2014. Quantitative generalizations for catchment sediment yield following forest logging. Water Resour. Res. 50, 8383–8402. https://doi.org/10.1002/2014WR015711.
Bedsworth, L., Cayan, D., Franco, G., Fisher, L., Ziaja, S., 2018. California's fourth climate change assessment: Statewide summary report. Sacramento, CA.
Borah, D.K., Yagow, G., Saleh, A., Barnes, P.L., Rosenthal, W., Krug, E.C., Hauck, L.M., 2006. Sediment and nutrient modeling for TMDL development and implementation. Trans ASABE 49, 967–986. 10.13031/2013.21742.
Bywater-Reyes, S., Segura, C., Bladon, K.D., 2017. Geology and geomorphology control suspended sediment yield and modulate increases following timber harvest in temperate headwater streams. J. Hydrol. 548, 754–769.
Bywater-Reyes, S., Bladon, K.D., Segura, C., 2018. Relative influence of landscape variables and discharge on suspended sediment yields in temperate mountain catchments. Water Resour. Res. 54, 5126–5142. https://doi.org/10.1029/2017WR021728.
Cafferata, P.H., Reid, L.M., 2013. Applications of long-term watershed research to forest management in California: 50 Years of Learning from the Caspar Creek Watershed Study. California Forestry Report No. 5. Sacramento: State of California, The Natural Resources Agency, Department of Forestry & Fire Protection. 114 p.
Callahan, R.P., Ferrier, K.L., Dixon, J., Dosseto, A., Hahm, W.J., Jessup, B.S., Miller, S.N., Hunsaker, C.T., Johnson, D.W., Sklar, L.S., Riebe, C.S., 2019. Arrested development: erosional equilibrium in the southern Sierra Nevada, California, maintained by feedbacks between channel incision and hillslope sediment production. GSA Bull. 131 (7–8), 1179–1202.
Carl, K.G., 1976. Sediment Discharge from highway cut-slopes in the lake tahoe basin, California, 1972–74 [WWW Document]. Water-Resour. Investig. Rep. 76–19 https://doi.org/10.3133/wri7619.
Certini, G., 2005. Effects of fire on properties of forest soils: a review. Oecologia 143, 1–10. https://doi.org/10.1007/s00442-004-1788-8.
Coats, R., Lewis, J., Alvarez, N., Arneson, P., 2016. Temporal and spatial trends in nutrient and sediment loading to Lake Tahoe, California-Nevada, USA. J. Am. Water Resour. Assoc. 52, 1347–1365. https://doi.org/10.1111/1752-1688.12461.
Cohen, S., Willgoose, G., Hancock, G., 2008. A methodology for calculating the spatial distribution of the area-slope equation and the hypsometric integral within a catchment. J. Geophys. Res. Earth Surf. 113 (F3) https://doi.org/10.1029/2007JF000820.
Cohn, T.A., Caulder, D.L., Gilroy, E.J., Zynjuk, L.D., Summers, R.M., 1992. The validity of a simple statistical model for estimating fluvial constituent loads: an empirical study involving nutrient loads entering Chesapeake Bay. Water Resour. Res. 28, 2353–2363. https://doi.org/10.1029/92WR01008.
Cole, R.P., Bladon, K.D., Wagenbrenner, J.W., Coe, D.B.R., 2020. Hillslope sediment production after wildfire and post-fire forest management in northern California. Hydrol. Process. 34, 5242–5259. https://doi.org/10.1002/HYP.13932.
Costa, A., Molnar, P., Stutenbecker, L., Bakker, M., Silva, T.A., Schlunegger, F., Lane, S. N., Loizeau, J.L., Girardclos, S., 2018. Temperature signal in suspended sediment export from an Alpine catchment. Hydrol. Earth Syst. Sci. 22, 509–528. https://doi.org/10.5194/hess-22-509-2018.
Czuba, J.A., Magirl, C.S., Czuba, C.R., Grossman, E.E., Curran, C.A., Gendaszek, A.S., Dinicola, R.S., 2011. Sediment load from major rivers into Puget Sound and its adjacent waters. US Department of the Interior, US Geological Survey. Fact Sheet 2011–3083.
Daly, C., Halbleib, M., Smith, J.I., Gibson, W.P., Doggett, M.K., Taylor, G.H., Curtis, J., Pasteris, P.P., 2008. Physiographically sensitive mapping of climatological temperature and precipitation across the conterminous United States. Int. J. Climatol.: J. Roy. Meteorol. Soc. 28 (15), 2031–2064. https://doi.org/10.1002/joc.1688.
Das, T., Maurer, E.P., Pierce, D.W., Dettinger, M.D., Cayan, D.R., 2013. Increases in flood magnitudes in California under warming climates. J. Hydrol. 501, 101–110. https://doi.org/10.1016/J.JHYDROL.2013.07.042.
DeBano, L.F., 1991. The effect of fire on soil properties, *In*: *Proceedings Management and Productivity of Western-Montane Forest Soils*. pp. 151–155.
Dettinger, M.D., Anderson, M.L., 2015. UC Davis San Francisco estuary and watershed science title storage in California's reservoirs and snowpack in this time of drought. 10.15447/sfews.2015v13iss2art1.
Eagan, S. M., Hunsaker, C. T., Dolanc, C. R., Lynch, M. E., & Johnson, C. R., 2007. Discharge and sediment loads at the Kings River experimental forest in the southern Sierra Nevada of California. In In: Furniss, M.; Clifton, C.; Ronnenberg, K., eds. 2007. Advancing the fundamental sciences: proceedings of the Forest Service National Earth Sciences Conference. Gen. Tech. Rep. PNW-GTR-689. Portland, OR: US Forest Service, Pacific Northwest Research Station: 217-224 (pp. 217-224).
Florsheim, J.L., Chin, A., Kinoshita, A.M., Nourbakhshbeidokhti, S., 2017. Effect of storms during drought on post-wildfire recovery of channel sediment dynamics and habitat in the southern California chaparral, USA. Earth Surf. Proc. Land. 42, 1482–1492. https://doi.org/10.1002/ESP.4117.
Gillespie, A.R., Clark, D.H., 2011. Glaciations of the Sierra Nevada, California, USA. Devel. Quat. Sci. 15, 447–462. https://doi.org/10.1016/B978-0-444-53447-7.00034-9.
Gillespie, A.R., Zehfuss, P.H., 2004. Glaciations of the Sierra Nevada, California, USA. Devel. Quat. Sci. 2, 51–62. https://doi.org/10.1016/S1571-0866(04)80185-4.
Gomi, T., Moore, R.D., Hassan, M.A., 2005. Suspended sediment dynamics in small forest streams of the pacific northwest. J. Am. Water Resour. Assoc. 41, 877–898. https://doi.org/10.1111/j.1752-1688.2005.tb03775.x.
Goudie, A.S., 2006. Global warming and fluvial geomorphology. Geomorphology 79, 384–394. https://doi.org/10.1016/j.geomorph.2006.06.023.
Grant, G.E., Wolff, A.L., 1991. Long-Term Patterns of Sediment Transport After Timber Harvest. IAHS Publ, Western Cascade Mountains, Oregon, USA.
Griffiths, P.G., Hereford, R., Webb, R.H., 2006. Sediment yield and runoff frequency of small drainage basins in the Mojave Desert, California and Nevada. US Department of the Interior, US Geological Survey. Fact Sheet 2006–3007.
Guan, B., Waliser, D.E., Ralph, F.M., Fetzer, E.J., Neiman, P.J., 2016. Hydrometeorological characteristics of rain-on-snow events associated with atmospheric rivers. Geophys. Res. Lett. 43, 2964–2973. https://doi.org/10.1002/2016GL067978.
Huning, L.S., AghaKouchak, A., 2018. Mountain snowpack response to different levels of warming. Proc. Natl. Acad. Sci. U.S.A. 115, 10932–10937.
Hunsaker, C. T., & Neary, D. G., 2012. Sediment loads and erosion in forest headwater streams of the Sierra Nevada, California. In In: Webb, Ashley A.; Bonell, Mike; Bren, Leon; Lane, Patrick NJ; McGuire, Don; Neary, Daniel G.; Nettles, Jami; Scott, David F.; Stednik, John; Wang, Yanhui, eds. Revisiting Experimental Catchment Studies in Forest Hydrology: Proceedings of a Workshop held during the XXV IUGG General Assembly in Melbourne, June-July 2011. IAHS Publication 353. United Kingdom: Wallingford: International Association of Hydrological Sciences. p. 195-204 (pp. 195-204).
Hunsaker, C.T., Safeeq, M., 2017. Kings River Experimental Watersheds stream discharge. Fort Collins, CO: Forest Service Research Data Archive. 10.2737/RDS-2017-0037.
Hunsaker, C.T., Whitaker, T.W., Bales, R.C., 2012. Snowmelt Runoff and Water Yield Along Elevation and Temperature Gradients in California's Southern Sierra Nevada1. J. Am. Water Resour. Assoc. 48, 667–678. https://doi.org/10.1111/J.1752-1688.2012.00641.X.
Jennings, C.W., Gutierrez, C., Bryant, W., Saucedo, G., Wills, C., 2010. Geologic Map of California [California Geological Survey, Geologic Data Map 2, scale 1: 750,000]. California Geological Survey, Sacramento, CA, US.
Johnson, D.W., Hunsaker, C.T., Glass, D.W., Rau, B.M., Roath, B.A., 2011. Carbon and nutrient contents in soils from the Kings River Experimental Watersheds, Sierra Nevada Mountains, California. Geoderma 160, 490–502. https://doi.org/10.1016/J.GEODERMA.2010.10.019.
Kattelmann, R., 1989. Hydrology of four headwater basins in the Sierra Nevada, in: Proceedings of the Symposium on Headwaters Hydrology. American Water Resources Association, Bethesda Maryland. 1989. p 141-147, 3 Fig, 3 Ref.
Kaufman, D.S., Porter, S.C., Gillespie, A.R., 2003. Quaternary alpine glaciation in Alaska, the Pacific Northwest, Sierra Nevada, and Hawaii. Devel. Quat. Sci. 1, 77–103. https://doi.org/10.1016/S1571-0866(03)01005-4.
Kemp, P., Sear, D., Collins, A., Naden, P., Jones, I., 2011. The impacts of fine sediment on riverine fish. Hydrol. Process. 25, 1800–1821. https://doi.org/10.1002/HYP.7940.
Klein, R.D., Lewis, J., Buffleben, M.S., 2012. Logging and turbidity in the coastal watersheds of northern California. Geomorphology 139–140, 136–144. https://doi.org/10.1016/J.GEOMORPH.2011.10.011.
Klos, P.Z., Link, T.E., Abatzoglou, J.T., 2014. Extent of the rain-snow transition zone in the western U.S. under historic and projected climate. Geophys. Res. Lett. 41, 4560–4568. https://doi.org/10.1002/2014GL060500.
Lana-Renault, N., Alvera, B., García-Ruiz, J.M., 2011. Runoff and Sediment Transport during the Snowmelt Period in a Mediterranean High-Mountain Catchment. 10.1657/1938-4246-43.2.213 43, 213–222. 10.1657/1938-4246-43.2.213.
Langlois, J.L., Johnson, D.W., Mehuys, G.R., 2005. Suspended sediment dynamics associated with snowmelt runoff in a small mountain stream of Lake Tahoe (Nevada). Hydrol. Process. 19, 3569–3580. https://doi.org/10.1002/hyp.5844.
Lewis, J., Mori, S.R., Keppeler, E.T., Ziemer, R.R., 2001. Impacts of logging on storm peak flows, flow volumes and suspended sediment loads in Caspar Creek, California. In: Mark S. Wigmosta and Steven J. Burges (eds.) Land Use and Watersheds: Human Influence on Hydrology and Geomorphology in Urban and Forest Areas. Water Science and Application Volume 2, American Geophysical Union, Washington, DC; 85-125.
Lorenz, D. L., 2015. smwrBase—An R package for managing hydrologic data, version 1.1. 1 (No. 2015-1202). US Geological Survey.
Lumley, T., Miller, A., 2020. Package 'LEAPS': Regression subset selection. R package version 3.
Lund J. R., 2011. Water Storage in California. California WaterBlog (https://californiawaterblog.com/2011/09/13/water-storage-in-california-2/)[last accessed 5/7/2022].
Lund J. R., 2014. Should California expand reservoir capacity by removing sediment? California WaterBlog (https://californiawaterblog.com/2014/06/09/should-california-expand-reservoir-capacity-by-removing-sediment/)[last accessed 5/7/2022].
Lydersen, J.M., Collins, B.M., Hunsaker, C.T., 2019. Implementation constraints limit benefits of restoration treatments in mixed-conifer forests. Int. J. Wildland Fire 28, 495–511. https://doi.org/10.1071/WF18141.
Mano, V., Nemery, J., Belleudy, P., Poirel, A., 2009. Assessment of suspended sediment transport in four alpine watersheds (France): Influence of the climatic regime. Hydrol. Process. 23, 777–792. https://doi.org/10.1002/hyp.7178.

Martin, S. E., Hunsaker, C. T., & Bales, R. C. (2009, December). Sediment Sources in four Small Mountain Streams In the Central Sierra Nevada, California. In AGU Fall Meeting Abstracts (Vol. 2009, pp. EP53D-0649).

Mayor, A.G., Bautista, S., Llovet, J., Bellot, J., 2007. Post-fire hydrological and erosional responses of a Mediterranean landscpe: Seven years of catchment-scale dynamics. CATENA 71, 68–75. https://doi.org/10.1016/J.CATENA.2006.10.006.

Minear, J.T., Kondolf, G.M., 2009. Estimating reservoir sedimentation rates at large spatial and temporal scales: a case study of California. Water Resour. Res. 45 https://doi.org/10.1029/2007WR006703.

Morehead, M.D., Syvitski, J.P., Hutton, E.W.H., Peckham, S.D., 2003. Modeling the temporal variability in the flux of sediment from ungauged river basins. Global Planet. Change 39, 95–110. https://doi.org/10.1016/S0921-8181(03)00019-5.

Mueller, E.R., Pitlick, J., 2013. Sediment supply and channel morphology in mountain river systems: 1. Relative importance of lithology, topography, and climate. J. Geophys. Res. Earth Surf. 118, 2325–2342. https://doi.org/10.1002/2013JF002843.

Mueller, E.R., Smith, M.E., Pitlick, J., 2016. Lithology-controlled evolution of stream bed sediment and basin-scale sediment yields in adjacent mountain watersheds, Idaho, USA. Earth Surf. Proc. Land. 41 (13), 1869–1883.

Neiman, P.J., Ralph, F.M., Wick, G.A., Lundquist, J.D., Dettinger, M.D., 2008. Meteorological characteristics and overland precipitation impacts of atmospheric rivers affecting the West Coast of North America based on eight years of SSM/I satellite observations. J. Hydrometeorol. 9, 22–47. https://doi.org/10.1175/2007JHM855.1.

Nolan, K.M., Lisle, T.E., Kelsey, H.M., 1987. Bankfull discharge and sediment transport in northwestern California, *In*: R. Beschta, T. Blinn, GE Grant, FJ Swanson, and GG Ice (Ed.), Erosion and Sedimentation in the Pacific Rim (Proceedings of the Corvallis Symposium, August 1987). International Association of Hydrological Sciences Pub. No. 165, p. 439-449.

Nolan, K.M., Hill, B.R., 1991. Suspended-sediment budgets for four drainage basins tributary to Lake Tahoe, California and Nevada, 1984–87 Water-Resources Investigations Report 91–4054. US Department of the Interior, US Geological Survey.

North, M.P., Stephens, S.L., Collins, B.M., Agee, J.K., Aplet, G., Franklin, J.F., Fulé, P.Z., 2015. Reform forest fire management: agency incentives undermine policy effectiveness. Science 1979 (349), 1280–1281.

O'Connor, J.E., Mangano, J.F., Anderson, S.W., Wallick, J.R., Jones, K.L., Keith, M.K., 2014. Geologic and physiographic controls on bed-material yield, transport, and channel morphology for alluvial and bedrock rivers, western Oregon. Bull. Geol. Soc. Am. 126, 377–397. https://doi.org/10.1130/B30831.1.

O'Geen, A.T., Safeeq, M., Wagenbrenner, J., Stacy, E., Hartsough, P., Devine, S., Tian, Z., Ferrell, R., Goulden, M., Hopmans, J.W., Bales, R., 2018. Southern Sierra Critical Zone Observatory and Kings River Experimental Watersheds: a synthesis of measurements, new insights, and future directions. Vadose Zone J. 17, 180081 https://doi.org/10.2136/vzj2018.04.0081.

Olsen, W.H., Wagenbrenner, J.W., Robichaud, P.R., 2021. Factors affecting connectivity and sediment yields following wildfire and post-fire salvage logging in California's Sierra Nevada. Hydrol. Process. 35, e13984.

Patric, J.H., Evans, J.O., Helvey, J.D., 1984. Summary of sediment yield data from forested land in the United States. J. Forest. 82, 101–104. https://doi.org/10.1093/JOF/82.2.101.

Phillips, C.B., Jerolmack, D.J., 2016. Self-organization of river channels as a critical filter on climate signals. Science 1979 (352), 694–697.

Podolak, C.J.P., Doyle, M.W., 2015. Reservoir sedimentation and storage capacity in the United States: management needs for the 21st century. J. Hydraul. Eng. 141, 02515001. https://doi.org/10.1061/(ASCE)HY.1943-7900.0000999.

R Core Team, 2020. R: A language and environment for statistical computing 3. R Foundation for Statistical Computing, Vienna, Austria.

Rachels, A.A., Bladon, K.D., Bywater-Reyes, S., Hatten, J.A., 2020. Quantifying effects of forest harvesting on sources of suspended sediment to an Oregon Coast Range headwater stream. For. Ecol. Manage. 466 https://doi.org/10.1016/j.foreco.2020.118123.

Rainato, R., Mao, L., García-Rama, A., Picco, L., Cesca, M., Vianello, A., Preciso, E., Scussel, G.R., Lenzi, M.A., 2017. Three decades of monitoring in the Rio Cordon instrumented basin: Sediment budget and temporal trend of sediment yield. Geomorphology 291, 45–56. https://doi.org/10.1016/J.GEOMORPH.2016.03.012.

Reuter, J.E., Miller, W.W., 2000. Chapter four aquatic resources, water quality, and limnology of lake tahoe and its upland watershed., in: Lake Tahoe Watershed Assessment. pp. 215–399.

Richardson, P.W., Wagenbrenner, J.W., Sutherland, D.G., Lisle, T.E., 2020. Measuring and modeling gravel transport at Caspar Creek, CA, to detect changes in sediment supply, storage, and transport efficiency. Water Resources Research 56, e2019WR026389. 10.1029/2019WR026389.

Richardson, P., Wagenbrenner, J., 2020. Supplemental bed load data for the North Fork of Caspar Creek, CA - Harvard Dataverse [WWW Document]. Harvard Dataverse V1. https://doi.org/10.7910/DVN/ZKYNQC.

Riebe, C.S., Kirchner, J.W., Granger, D.E., Finkel, R.C., 2000. Erosional equilibrium and disequilibrium in the Sierra Nevada, inferred from cosmogenic 26Al and 10Be in alluvial sediment. Geology 28 (9), 803–806.

Riebe, C.S., Kirchner, J.W., Granger, D.E., Finkel, R.C., 2001. Minimal climatic control on erosion rates in the Sierra Nevada. Calif. Geol. 29 (5), 447–450.

Robichaud, P.R., Wagenbrenner, J.W., Brown, R.E., Wohlgemuth, P.M., Beyers, J.L., 2008. Evaluating the effectiveness of contour-felled log erosion barriers as a post-fire runoff and erosion mitigation treatment in the western United States. Int. J. Wildland Fire 17, 255–273. https://doi.org/10.1071/WF07032.

Robichaud, P.R., Jordan, P., Lewis, S.A., Ashmun, L.E., Covert, S.A., Brown, R.E., 2013. Evaluating the effectiveness of wood shred and agricultural straw mulches as a treatment to reduce post-wildfire hillslope erosion in southern British Columbia, Canada. Geomorphology 197, 21–33. https://doi.org/10.1016/J.GEOMORPH.2013.04.024.

Robichaud, P.R., Wagenbrenner, J.W., Pierson, F.B., Spaeth, K.E., Ashmun, L.E., Moffet, C.A., 2016. Infiltration and interrill erosion rates after a wildfire in western Montana, USA. CATENA 142, 77–88. https://doi.org/10.1016/J.CATENA.2016.01.027.

Safeeq, M., Hunsaker, C.T., 2016. Characterizing runoff and water yield for headwater catchments in the Southern Sierra Nevada. J. Am. Water Resour. Assoc. 52, 1327–1346. https://doi.org/10.1111/1752-1688.12457.

Safeeq, M., Shukla, S., Arismendi, I., Grant, G.E., Lewis, S.L., Nolin, A., 2016. Influence of winter season climate variability on snow–precipitation ratio in the western United States. Int. J. Climatol. 36, 3175–3190. https://doi.org/10.1002/JOC.4545.

Safeeq, M., Grant, G.E., Lewis, S.L., Hayes, S.K., 2020. Disentangling effects of forest harvest on long-term hydrologic and sediment dynamics, western Cascades, Oregon. J. Hydrol. 580 https://doi.org/10.1016/j.jhydrol.2019.124259.

Schleiss, A.J., Franca, M.J., Juez, C., de Cesare, G., 2016. Reservoir sedimentation. J. Hydraul. Res. 54, 595–614. https://doi.org/10.1080/00221686.2016.1225320.

Sierra Nevada Conservancy, 2014. The State of the Sierra Nevada's Forests. Sierra Nevada Conservancy, 11521. (Accessed 6 August 2022).

Simon, A., Langendoen, E., Bingner, R., Wells, R., Heins, A., Jokay, N., Jaramillo, I., 2003. Lake Tahoe Basin Framework Implementation Study: Sediment Loadings and Channel Erosion. USDA-ARS National Sedimentation Laboratory Research Report. No 39, 377–pp.

Singh, O., Sarangi, A., Sharma, M.C., 2008. Hypsometric integral estimation methods and its relevance on erosion status of North-Western Lesser Himalayan watersheds. Water Resour. Manage. 22, 1545–1560. https://doi.org/10.1007/s11269-008-9242-z.

Solgi, A., Najafi, A., Ezzati, S., Ferencik, M., 2016. Assessment of ground-based skidding impacts on the horizontally rate and extent of soil disturbance along the margin of the skid trail. Ann. For. Sci. 73, 513–522. https://doi.org/10.1007/S13595-016-0544-7/TABLES/8.

Stacy, E.M., Hart, S.C., Hunsaker, C.T., Johnson, D.W., Berhe, A.A., 2015. Soil carbon and nitrogen erosion in forested catchments: Implications for erosion-induced terrestrial carbon sequestration. Biogeosciences 12, 4861–4874. https://doi.org/10.5194/bg-12-4861-2015.

Stallman, J.D., Bowers, R.J., Cabera, N.C., Real de Asua, R., Wooster, J.K., 2005. Sediment dynamics in the Upper McKenzie River Basin, Central Oregon Cascade Range. AGU Fall Meeting abstracts #H51E-0411.

Strahler, A.N., 1952. Hypsometric (area-altitude) analysis of erosional topography. Geol. Soc. Am. Bull. 63, 1117–1142.

Swank, W.T., Vose, J.M., Elliott, K.J., 2001. Long-term hydrologic and water quality responses following commercial clearcutting of mixed hardwoods on a southern Appalachian catchment. For. Ecol. Manage. 143, 163–178. https://doi.org/10.1016/S0378-1127(00)00515-6.

Syvitski, J.P.M., Milliman, J.D., 2007. Geology, geography, and humans battle for dominance over the delivery of fluvial sediment to the coastal ocean. J. Geol. 115, 1–19. https://doi.org/10.1086/509246/SUPPL_FILE/115101APA.PDF.

Turowski, J.M., Badoux, A., Rickenmann, D., 2011. Start and end of bedload transport in gravel-bed streams. Geophys. Res. Lett. 38 https://doi.org/10.1029/2010GL046558.

United States Environmental Protection Agency, 2016a. Water Quality Assessment and TMDL Information | Water Quality Assessment and TMDL Information | US EPA [WWW Document]. URL https://iaspub.epa.gov/waters10/attains_index.home (accessed 1.25.22).

United States Environmental Protection Agency, 2016b. California Water Quality Assessment Report | Water Quality Assessment and TMDL Information | US EPA [WWW Document]. URL https://iaspub.epa.gov/waters10/attains_state.control?p_state=CA (accessed 1.25.22).

Vachtman, D., Mitchell, N.C., Gawthorpe, R., 2013. Morphologic signatures in submarine canyons and gullies, central USA Atlantic continental margins. Mar. Pet. Geol. 41, 250–263. https://doi.org/10.1016/J.MARPETGEO.2012.02.005.

Verstraeten, G., Poesen, J., 2001. The importance of sediment characteristics and trap efficiency in assessing sediment yield using retention ponds. Physics and Chemistry of the Earth, Part B. Hydrology Oceans Atmos. 26, 83–87. https://doi.org/10.1016/S1464-1909(01)85019-X.

Vivoni, E.R., Di Benedetto, F., Grimaldi, S., Eltahir, E.A., 2008. Hypsometric control on surface and subsurface runoff. Water Resour. Res. 44, 12502. https://doi.org/10.1029/2008WR006931.

Wagenbrenner, J.W., Dralle, D.N., Safeeq, M., Hunsaker, C.T., 2021a. The Kings River Experimental Watersheds, infrastructure and data. Hydrol. Process. 35, e14142.

Wagenbrenner, J.W., Ebel, B.A., Bladon, K.D., Kinoshita, A.M., 2021b. Post-wildfire hydrologic recovery in Mediterranean climates: A systematic review and case study to identify current knowledge and opportunities. J. Hydrol. 602, 126772 https://doi.org/10.1016/j.jhydrol.2021.126772.

Westerling, A.L., Hidalgo, H.G., Cayan, D.R., Swetnam, T.W., 2006. Warming and earlier spring increase Western U.S. forest wildfire activity. Science (1979) 313, 940–943.

Wise, D.R. and O'Connor, J., 2016. A spatially explicit suspended-sediment load model for Western Oregon (No. 2016-5079). US Geological Survey. 10.3133/sir20165079.

Wohlgemuth, P.M., Hubbert, K.R., Robichaud, P.R., 2001. The effects of log erosion barriers on post-fire hydrologic response and sediment yield in small forested watersheds, southern California. Hydrol. Process 15, 3053–3066. https://doi.org/10.1002/hyp.391.